Progress in Physical Geography

Glacier melt: a review of processes and their modelling
Regine Hock

The online version of this article can be found at:
http://ppg.sagepub.com/cgi/content/abstract/29/3/362

Additional services and information for *Progress in Physical Geography* can be found at:

Email Alerts: http://ppg.sagepub.com/cgi/alerts

Subscriptions: http://ppg.sagepub.com/subscriptions

Reprints: http://www.sagepub.com/journalsReprints.nav

Permissions: http://www.sagepub.com/journalsPermissions.nav

Citations (this article cites 29 articles hosted on the
SAGE Journals Online and HighWire Press platforms):
http://ppg.sagepub.com/cgi/content/refs/29/3/362

Glacier melt: a review of processes and their modelling

Regine Hock

Institute for Atmospheric and Climate Science Swiss Federal Institute of Technology, CH-8057 Zürich, Switzerland, and Department of Physical Geography and Quaternary Geology, Stockholm University, SE-106 91 Stockholm, Sweden

Abstract: Modelling ice and snow melt is of large practical and scientific interest, including issues such as water resource management, avalanche forecasting, glacier dynamics, hydrology and hydrochemistry, as well as the response of glaciers to climate change. During the last few decades, a large variety of melt models have been developed, ranging from simple temperature-index to sophisticated energy-balance models. There is a recent trend towards modelling with both high temporal and spatial resolution, the latter accomplished by fully distributed models. This review discusses the relevant processes at the surface-atmosphere interface, and their representation in melt models. Despite considerable advances in distributed melt modelling there is still a need to refine and develop models with high spatial and temporal resolution based on moderate input data requirements. While modelling of incoming radiation in mountain terrain is relatively accurate, modelling of turbulent fluxes and spatial and temporal variability in albedo constitute major uncertainties in current energy-balance melt models, and thus need further research.

Key words: distributed models, energy balance, glacier melt, modelling, temperature-index models.

I Introduction

1 Background

Glacier ice and snow cover exert a major control on the dynamics of the Earth with respect to both climate and hydrology. From a climatologic point of view, snow and ice play an important role, interacting with the atmosphere over a range of spatial and temporal scales involving complex and sensitive feedback mechanisms. From a hydrological perspective, glaciers represent important water resources, contributing significantly to streamflow. Glaciers exert a considerable influence on catchment hydrology, especially in mountain areas, by temporarily storing water as snow and ice on many timescales (Jansson *et al.*, 2003). Typical characteristics of glacier runoff involve marked melt-induced diurnal cyclicity and a concentration of annual flow during the melt season (Figure 1). An increasing demand for fresh water has stimulated the need to predict melt-derived streamflow as a basis for efficient water resource management, with respect to issues such as water supply, management of hydro-electric facilities and flood forecasting. The success of modelling glacier-derived runoff strongly depends on the formulation of the melt processs. Melt modelling has tradition-ally been motivated by runoff forecasts, but in
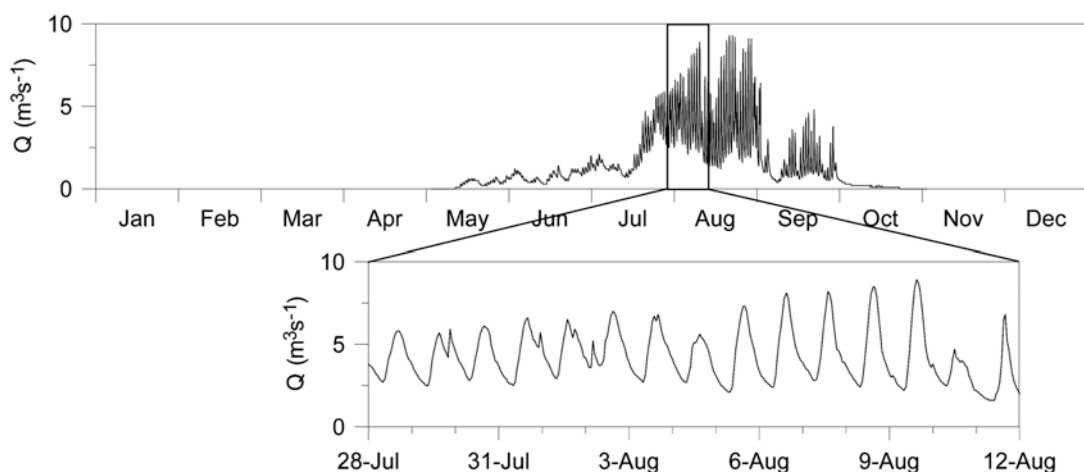
Figure 1 Hydrograph of hourly discharge at Vernagtferner, Austria, 1990, displaying seasonal and diurnal variations typical of glacier regimes
Source: data from Commission for Glaciology of the Bavarian Academy of Science, Munich.

recent years interest has risen, in particular in spatially distributed estimates of snow and ice melt for many other purposes. These include avalanche forecasts, assessment of the contribution of melting ice to sea-level rise, as well as studies in glacier dynamics, hydrochemistry and erosion.

Meltwater production, in particular from snow cover, has received extensive examination in terms of both measurements and modelling. There is a complete hierarchy of melt models relating ablation to meteorological conditions, varying greatly in complexity and scope. These range from models based on the detailed evaluation of the surface energy fluxes (*energy-balance models*) to models using air temperature as the sole index of melt energy (*temperature-index models*). Much work has been done at the point scale. However, promoted by increased availability of digital terrain models and computational power, increasing efforts have been devoted to areal melt modelling using fully distributed models. In addition, there is a trend towards high temporal resolution modelling (e.g., with hourly time steps). The latter is essential

for predicting peak flows in glacierized or snow-covered basins. High spatial resolution is needed to account for the large spatial heterogeneity with respect to ice and snow melt typically encountered in steeply sided terrain as a result of the effects of surrounding topography.

Previous reviews have addressed individual aspects of melt and its modelling: Lang (1986) and Röthlisberger and Lang (1987) present an overview of glacier melt and discharge processes. An exhaustive review of radiation and turbulent heat transfer at a snow surface is given by Male and Granger (1981). Male (1980) and Dozier (1987) summarize the processes of snow melt and hydrology. Kirnbauer *et al.* (1994) focus on distributed snow models. Recent trends in temperature-index melt modelling are discussed in Hock (2003). This review considers recent advances in the simulation of melt, focusing on glaciers and distributed modelling. The relevant processes involved in energy exchange at the glacier surface are discussed with respect to their representation in melt models. Emphasis is on models suitable for

operational purposes, hence on methods requiring moderate data input.

2 Historical overview

The relationship between glacier behaviour and climate has long been a central issue in glaciology. This applies in particular to mountainous regions, where people have experienced damage to farmlands and villages either by direct advance of a glacier or by glacier outburst floods (e.g., Finsterwalder, 1897; Hoinkes, 1969). Early studies attempted to investigate the causes of glacier fluctuations. Walcher (1773) was one of the first to propose that glacier fluctuations are caused by variations in climatic conditions. Finsterwalder and Schunk (1887) suggested a close relation between air temperature and ablation. Hess (1904) recognized radiation as the most important source of energy for melt. Ångström (1933) stressed the importance of temperature, radiation and wind as agents for melting.

Pioneering work concerning the details of energy exchange between the atmosphere and a glacier surface was performed in the Nordic countries. In the 1920s, Ahlmann related ablation measurements to simultaneous meteorological observations and he derived the first empirical formula for the computation of ablation from known values of incident radiation, air temperature and wind velocity (Ahlmann, 1935; 1948). Sverdrup's study in West Spitzbergen in 1934 provided the foundation for most glacier and snow cover energy transfer studies to follow (Sverdrup, 1935; 1936). He computed a complete energy balance, although primarily focusing on the turbulent heat fluxes. He was the first to apply gradient flux techniques to ice and snow. In the 1940s, Wallén (1949) conducted a detailed glaciometeorological experiment during six successive summers on Kårsaglacier in northern Sweden. He concluded that studies of glacier variations should deal with changes in the total volume of glaciers and not only with front variations.

In the Alps, early comprehensive investigations to quantify the relationships between glacier and climate fluctuations, and to assess the water balance of glacierized catchments, were started in the 1930s (Lütschg-Loetscher, 1944). Hoeck (1952) focused on snow melt and systematically investigated the climatic and topographic variables determining the energy exchange of a snow cover. Detailed investigations of the radiation budget over glacier surfaces were initiated in 1938 at Sonnblick (3100 m a.s.l.) in the Austrian Alps and further developed in the 1950s (Sauberer and Dirmhirn, 1952). A comprehensive study of water, ice and energy budgets was started on several glaciers in Oetztal, Austria, in 1948 and greatly expanded during the International Hydrological Decade in the 1950s (Hoinkes and Untersteiner, 1952; Hoinkes, 1955), during which several long-term mass balance series were initiated (Hoinkes and Steinacker, 1975; Reinwarth and Escher-Vetter, 1999).

Although restricted to snow surfaces, a general and very thorough discussion of snow cover energy exchange and melt processes from both a theoretical and practical viewpoint was given by the Corps of Engineers (1956) and Kuzmin (1961), based on exhaustive studies in the USA and the former Soviet Union, respectively. Their work contained generalized snow melt equations based on theoretical and empirical considerations and formed the basis of many of the snow and ice melt models which were to follow.

In the 1960s, the first computer simulation models of accumulation and ablation processes were developed (Anderson, 1972; Crawford, 1973; WMO, 1986). This early stage of mass balance modelling pertained to snow covers and generally aimed at providing the meltwater input for watershed models. Since then, a large variety of snow models ranging from simple temperature-index models (e.g., Anderson, 1973; Braun and Aellen, 1990) to sophisticated energy-balance models, including simulation of the internal state of the snow cover, have been developed (e.g., Brun *et al.*, 1989). Modelling attempts focusing on

glaciers and ice sheets began in connection with the growing concern about potentially enhanced greenhouse warming and the effects on global sea level (e.g., Braithwaite and Olesen, 1990a; Oerlemans and Fortuin, 1992), as well as an increased interest in tapping glacial water for hydroelectric purposes (e.g., Braithwaite and Thomsen, 1989; van de Wal and Russel, 1994). The most recent development concerns the incorporation of remote sensing data into melt models, providing a particularly useful tool in basins inaccessible for detailed ground surveys (e.g., Seidel and Martinec, 1993; Reeh *et al.*, 2002). In addition, much effort is focused on enhancing the spatial and temporal resolution of melt models by moving from point-scale to distributed modelling and from, for example, daily time steps to hourly time steps (Burlando *et al.*, 2002).

3 Characteristics of snow and ice relevant to melt

Glacier melt is determined by the energy balance at the glacier-atmosphere interface, which is controlled by the meteorological conditions above the glacier and the physical properties of the glacier itself. Glacier-atmosphere interactions are complex. The atmosphere supplies energy for melt, while atmospheric conditions are modified by the presence of snow and ice due to the specific properties of snow and ice and their high temporal variability. In general, snow and ice are characterized by (Male, 1980; Kuhn, 1984):

• fixed surface temperatures during melting (0°C);
• penetration of shortwave radiation;
• high and largely variable albedo;
• high thermal emissivity;
• variable surface roughness.

Because the surface temperature of a melting snow or ice surface cannot exceed 0°C, strong temperature gradients can develop in the air immediately above the surface. Consequently, during the melt season, the air is generally stably stratified, thus suppressing

turbulence. Gradients may reach more than 5 K m^{-1} within the first 2 m above the surface (Holmgren, 1971; Oerlemans and Grisogono, 2002). Temperature stratification combined with typical glacier surface slopes induces gravity flows (Ohata, 1989; van den Broeke, 1997). On small valley glaciers, this glacier wind typically reaches a maximum between 0.5 and 3 m above the surface. Due to the fact that surface temperature cannot increase beyond 0°C, turbulent fluxes at some point become independent of radiation (Holmgren, 1971; Greuell *et al.*, 1997).

The vapour pressure of a melting surface is 6.11 hPa. This relatively low value favours vapour pressure gradients towards the surface, and leads to condensation. Since the latent heat of evaporation (2.501×10^6 J kg^{-1} at 0°C) is 7.5 times larger than the latent heat of fusion required for melting of snow and ice (0.334×10^6 J kg^{-1}), condensation can be an important energy source (e.g., Sverdrup, 1935; de Quervain, 1951; Orvig, 1954). With reversed vapour gradients, evaporation occurs, significantly reducing the energy available for melt due to the high energy consumption involved in evaporation. Thus, the process of evaporation is considered to play an important role in maintaining low-latitude glaciers and the present ice sheets (Ohmura *et al.*, 1994).

Shortwave radiation penetrates ice and snow to a depth of about 10 m and 1 m, respectively, depending on their physical properties (Warren, 1982; Oke, 1987). Only about 1–2% of global radiation (shortwave incoming radiation) penetrates into a snow cover (Ohmura, 1981; Konzelmann and Ohmura, 1995), and due to the exponential decline of transmitted radiation most of the energy is absorbed in the first few mm below the surface. However, the process is important for heating the snow cover during pre-melt periods and for internal melting, which may even occur when the surface is frozen due to net outgoing longwave radiation (Holmgren, 1971). La Chapelle (1961) observed measurable amounts of snow

melting as deep as 20 cm below the summer surface. On Peyto Glacier, 20% of the daily snow melt took place internally as a result of penetration of shortwave radiation (Föhn, 1973). Winther *et al.* (1996) attributed subsurface melt layers exceeding 0.5 m in thickness in blue ice areas in Antarctica to this process. On glacier ice, internal melting is important for the formation of a low-density 'weathering crust' in the top layer of the ice (Müeller and Keeler, 1969; Munro, 1990).

Snow is generally characterized by a higher albedo than ice, varying roughly between 0.7 and 0.9 compared to 0.3 to 0.5 for ice (Paterson, 1994). In the infrared part of the spectrum, both snow and ice behave as almost perfect black-bodies (Kondratyev, 1969), with emissivities of about 0.98–0.99 for snow and 0.97 for ice (Müller, 1985). The thermal conductivity of typical snow layers is less than one tenth of that of ice (Table 1), rendering snow a particularly good insulator. Nevertheless, snow temperatures near the surface can drop rapidly during periods of no melt, occurring in particular at high altitudes on clear nights. Combined with high albedo and high thermal emissivity, snow represents a radiative sink during such periods. Its thermal insulating properties prevent efficient compensation of these radiative losses. Snow and ice melt at 0°C. However, melting will not necessarily occur at air temperatures of 0°C, since melt is determined by the surface energy balance which in turn only indirectly is affected by air temperature (Kuhn, 1987).

Table 1   Some properties of snow and ice at 0°C (from Oke, 1987; Paterson, 1994)

	Typical density kg m^{-3}	Specific heat capacity J kg^{-1} K^{-1}	Thermal conductivity W m^{-1} K^{-1}
Fresh snow	50–150	2009	0.08
Old snow	200–500	2009	0.42
Ice	900	2097	2.1

II Energy-balance melt models

A physically based approach to compute melt involves the assessment of the energy fluxes to and from the surface. At a surface temperature of 0°C, any surplus of energy at the surface-air interface is assumed to be used immediately for melting. The energy balance in terms of its components is expressed as:

$$Q_N + Q_H + Q_L + Q_G + Q_R + Q_M = 0 \qquad (1)$$

where Q_N is net radiation, Q_H is the sensible heat flux, Q_L is the latent heat flux (Q_H and Q_L are referred to as turbulent heat fluxes), Q_G is the ground heat flux, i.e., the change in heat of a vertical column from the surface to the depth at which vertical heat transfer is negligible, Q_R is the sensible heat flux supplied by rain and Q_M is the energy consumed by melt. As commonly defined in glaciology, a positive sign indicates an energy gain to the surface, a negative sign an energy loss. Melt rates, M are then computed from the available energy by:

$$M = \frac{Q_M}{\rho_w L_f} \qquad (2)$$

where ρ_w denotes the density of water and L_f the latent heat of fusion. Energy-balance models fall into two categories: point studies and distributed models. The former assess the energy budget at one location, usually the site of a climate station. The latter involve estimating the budget over an area, usually on a square grid.

Examples of point studies on glaciers are given in Table 2 complementing similar summaries by, for example, Ohmura *et al.* (1992) and Willis *et al.* (2002). Complete energy budget measurements are seldom available and if so only over short periods of time due to the enormous equipment and maintenance requirements. Hence, methods of computing the energy budget components from standard meteorological observations have been developed and applied in most studies (see Table 2 for references). Despite simplifying assumptions inherent to these methods, they have provided reliable

Table 2 Point energy-balance studies on Alpine valley glaciers. Net radiation Q_N, sensible heat flux Q_H, latent heat flux Q_L, ice heat flux Q_G and the energy for melt Q_M (here defined as negative) are given in W m^{-2}. Values in brackets are in % of total energy source or sink. The energy balance does not necessarily balance if Q_M is obtained from ablation measurements instead of from closing the energy balance

Location, m a.s.l., surface type	Period (d = days)	Q_N	Q_H	Q_L	Q_G	Q_M	Reference
Vernagtferner 2970 m, ice	45 d in Aug + Sep 1950–53	143 (84)	23 (14)	4 (2)	0 (0)	−170 (−100)	Hoinkes, 1955
Kesselwandferner 3240 m, snow	20 d in 1958	43 (67)	21 (33)	−1 (−2)		−64 (−98)	Ambach and Hoinkes, 1963
Blue Glacier 2050 m	12.7.–20.8.1958	85 (63)	50 (37)	−3 (−2)		−132 (−98)	La Chapelle, 1959
Aletschglacier 2220 m, ice	2.–27.8.1965	129 (71)	38 (21)	14 (8)		−181 (−100)	Röthlisberger and Lang, 1987
Aletschglacier 3366 m, snow	3.–19.8.1973	44 (92)	4 (8)	−3 (−6)		−45 (−94)	Röthlisberger and Lang, 1987
Worthington Glacier Alaska, ice	16.7.–1.8.1967	127 (51)	68 (29)	47 (20)		−224 (−100)	Streten and Wendler, 1968
Peytoglacier 2510 m	14 d in July 1970	80 (44)	87 (48)	15 (8)		−181 (−100)	Föhn, 1973
Hodges Glacier South Georgia, 460 m	1.11.1973–4.4.1974	47 (54)	42 (46)	−3 (−3)		−86 (−97)	Hogg et al., 1982
St Sorlin Glacier 2700 m	11 d in summer	32 (57)	24 (43)	−4 (−7)		−53 (−93)	Martin, 1975
Hintereisferner ice	10 d in 1986	191 (90)	22 (10)	−4 (−2)		−209 (−98)	Greuell and Oerlemans, 1987
Ivory Glacier, New Zealand, 1500 m	53 d in Jan–Feb 1972/73	76 (52)	44 (30)	23 (16)	*	−147 (−100)	Hay and Fitzharris, 1988
Storglaciären 1370 m, ice	19.7.–27.8.1994	73 (66)	33 (30)	5 (5)	−3 (−3)	−122 (−97)	Hock and Holmgren, 1996
Paterze glacier 2205 m, ice	24.6.–9.9.1994	180 (74)	51 (21)	11 (5)		−242 (−100)	van den Broeke, 1997
Zongo Glacier 5150 m, ice/snow	9/1996–8/1997	17 (65)	6 (23)	−17 (−65)	3 (12)	−9 (−35)	Wagnon et al., 1999
Morteratschgletscher** 2100 m, ice/snow	1.10.1995–30.9.1998	152 (80)	31 (16)	8 (4)		−191 (−100)	Oerlemans, 2000
Koryto Glacier, Kamchatka, 840 m, snow	10.8.–8.9.2000	43 (33)	59 (44)	31 (33)		−133 (−100)	Konya et al., 2004

*Rain supplied 4 W m^{-2} (2%).
**Only when melting occurred.

estimates of ablation. In general, most of the energy used for melt is supplied by radiation, followed by the sensible heat flux and only a minor fraction is derived from latent heat (Table 2). The importance of net radiation relative to the turbulent fluxes tends to increase with altitude, as a result of reduced turbulent fluxes due to the vertical lapse rates of air temperature and vapour pressure (Röthlisberger and Lang, 1987).

Direct comparisons of different studies should be treated with caution, as most studies extend only over timescales of days or weeks rather than for the entire ablation season. The relative importance of the different components of the energy balance depends strongly on weather conditions and their relative contributions may change during the melt season. On Devon Island Ice Cap, Holmgren (1971) found relative contributions of net radiation, sensible heat flux and the latent heat flux of 70, 20 and 8% on clear-sky days with light winds. On overcast days with strong winds, the percentages changed to 44, 46 and 10%, respectively. In addition, different accuracy in instrumentation and methods of computation restrict such direct comparison. Distributed, grid-based energy-balance studies over ice and snow are comparatively scarce (Table 3). The main challenge for

distributed studies is the extrapolation of input data and energy budget components to the entire grid.

1 Net radiation

Net all-wave radiation of a surface is the difference between the incoming and outgoing energies absorbed or emitted by the surface (Kondratyev, 1965). Traditionally, radiation is classified as shortwave or longwave. The former covers the wavelength range of approximately 0.15–4 μm and predominantly originates directly from the sun, whereas the longwave radiation refers to the spectrum of 4–120 μm and is mainly thermal radiation of terrestrial and atmospheric origin. In mountainous regions, the radiative fluxes, in particular the direct sun radiation, vary considerably in space and time as a result of the effects of slope, aspect and effective horizon. These effects include reduction of incoming radiation by obstruction of the sky as well as reflection and emission of the surrounding slopes. Thus, the radiation balance may be written as (Kondratyev, 1965):

$$Q_N = (I + D_s + D_t)(1 - \alpha) + L_s^\downarrow + L_t^\downarrow + L\uparrow \quad (3)$$

where I is direct solar radiation, D_s is diffuse sky radiation, D_t is reflected radiation from the surrounding terrain ($I + D_s + D_t$ is

Table 3   Grid-based energy-balance melt models applied to mountain glaciers and snow-covered mountain areas

Location	Time resolution	Grid spacing	Reference
Glaciers			
Rhonegletscher (18.7 km²)	day	100 m	Funk, 1985
Vernagtferner (9.1 km²)	half-hour	100 m	Escher-Vetter, 1985b
Haut Glacier d' Arolla (6.3 km²)	hour	20 m	Arnold *et al.*, 1996
Storglaciären (3.1 km²)	hour	30 m	Hock and Noetzli, 1997
Moteratschgletscher (17.2 km²)	hour	25 m	Klok and Oerlemans, 2002
Snow			
Längental, Austria (9 km²)	hour	25 m	Blöschl *et al.*, 1991
Tedorigawa basin, Japan (247 km²)	day	540 × 469 m	Ujihashi *et al.*, 1994
Mount Iwate, Japan (11 km²)	hour	125 m	Ohta, 1994
Davos (16 km²)	day	25 m	Plüss, 1997

referred to as global radiation), α is albedo, $L_s^\downarrow$ is longwave sky radiation, $L_t^\downarrow$ is longwave radiation from the surrounding terrain and $L\uparrow$ is the emitted longwave radiation. Measurements of net radiation on glaciers are seldom available, and it is therefore necessary to parameterize the individual components.

2 Global radiation

Upon entering the atmosphere, solar radiation is partioned into direct and diffuse components. This is mainly due to scattering by air molecules, scattering and absorption by liquid and solid particles and selective absorption by water vapour and ozone, all processes having different wavelength dependencies. Besides atmospheric conditions and clouds, site-specific characteristics such as slope angle and aspect are also crucial for the computation of shortwave radiation in complex topography. Potential clear-sky direct solar radiation on an inclined surface I_c can be expressed by (e.g., Iqbal, 1983):

$$I_c = I_0 \left(\frac{R_m}{R} \right)^2 \psi_a^{\frac{P}{P_0 \cos z}} \cos\theta \qquad (4)$$

where I_0 is the solar constant ($\sim$1368 W m^{-2}), R is the sun-Earth distance (with subscript m refering to the mean), ψ_a is the atmospheric clear-sky transmissivity, P is atmospheric pressure, P_0 is mean atmospheric pressure at sea level, Z is the local zenith angle and θ is the angle of incidence between the slope-normal and the solar beam. A widely used solution for the incidence angle is given by Garnier and Ohmura (1968):

$$\cos\theta = \cos\beta \cos Z + \sin\beta \sin Z \\ \cos(\varphi_{sun} - \varphi_{slope}) \qquad (5)$$

where β is the slope angle, Z is the zenith angle and φ_{sun} and φ_{slope} are the solar azimuth and the slope azimuth angles, respectively. The zenith angle can be approximated as a function of latitude, solar declination and hour angle (e.g., Iqbal, 1983). Atmospheric attenuation of shortwave radiation can be described by Bouguer's law (also called Lambert's or Beer's law) and is proportional to the atmospheric pathlength and the initial radiation flux. In atmospheric models, this process is often parameterized by using different transmission coefficients for the most attenuative molecules and aerosols (e.g., Dozier, 1980). Transmissivities tend to be highest in winter and lowest in summer and tend to increase with latitude due to the lower atmospheric water vapour and dust content both in winter and at high latitudes. Clear-sky transmissivities vary between 0.6 and 0.9 (Oke, 1987). The amount of diffuse radiation depends largely on atmospheric conditions. The fractions of diffuse radiation to global radiation ranged from 36 to 51% in spring and 24 to 41% in summer at eight stations between latitudes of 40° and 60° (Kondratyev, 1969). At the ETH camp in Greenland, 40% of global radiation was diffuse on average during the summer months (Konzelmann and Ohmura, 1995). On clear-sky days this portion ranged from 13 to 17%. Holmgren (1971) reported 16% of global radiation as diffuse on Devon Ice Cap and Ohmura (1981) found 15 to 21% on Axel Heiberg Island.

In complex topography diffuse radiation originates from two sources – the sky and the surrounding topography – and consists of three components:
1. radiation that is initially scattered out of the beam by molecules and aerosols (sky radiation);
2. backscattered radiation, or the global radiation that is reflected by the snow surface and subsequently redirected downward by scattering and reflection in the atmosphere;
3. radiation reflected from adjacent slopes.

Consequently, surrounding topography affects the amount of diffuse radiation in two opposing ways: sky radiation is reduced as part of the sky is obscured, while diffuse radiation is enhanced by reflection from adjacent slopes. The backscattered component

strongly depends on albedo and it is greatly increased by the presence of snow due to enhanced multiple reflections between the ground and the atmosphere.

Clear-sky diffuse radiation is significantly anisotropic (Kondratyev, 1969). The intensity is greatest in the direction of the sun and near the horizon because of the greater optical thickness of the atmosphere at large zenith angles. This effect is considered in the radiation model by Dozier (1980). However, most melt models assume isotropy. This simplification is acceptable in most applications because diffuse radiation is most anisotropic for clear skies, when diffuse radiation is relatively low, and is nearly isotropic under overcast conditions (Garnier and Ohmura, 1968), when diffuse radiation tends to be high.

Many theoretical and empirical formulae to calculate diffuse radiation have been proposed (e.g., List, 1966; Wesley and Lipschutz, 1976). Diffuse sky irradiance onto an inclined surface is given by (Kondratyev, 1965):

$$D_s = \int_0^{2\pi} \int_{h(\varphi)}^{\pi/2} D(h, \varphi) \cos\theta \cos h \, dh \, d\varphi \quad (6)$$

where $D(h,\varphi)$ is the radiance from the direction determined by the angular height h relative to the horizontal plane and the azimuth angle φ, $h(\varphi)$ is the lowest angular height of the point in the sky unobstructed by topography in the azimuth φ and θ is the angle between the vector normal to the slope and an arbitrary direction. Most melt models refrain from integrating diffuse radiation over azimuth and zenith angles, and prefer a simpler so-called view-factor relationship to account for the effects of topography. The view-factor V_f is related to the fraction of the hemisphere unobstructed by surrounding slopes and can be approximated by:

$$V_f = \cos^2(H) \quad (7)$$

where H is the average horizon angle (Marks and Dozier, 1992). A widely used simplification is given by Kondratyev (1969) and applied, for example, by Arnold *et al.* (1996):

$$V_f = \cos^2(\beta/2) \quad (8)$$

with β the slope of the surface. Strictly speaking, this approximation only refers to a sloping surface without surrounding obstructions. Funk (1985) has shown that on Rhonegletscher results differed by roughly $\pm 10\%$ from those obtained by numerical integration of the horizon angle. Diffuse radiation on the inclined surface including the effects of topography can be approximated by

$$D = D_0 V_f + \alpha_m G(1 - V_f) \quad (9)$$

where D_0 is diffuse sky radiation of an unobstructed sky, G is global radiation and α_m is the mean albedo of the surroundings. The first term refers to sky radiation, the second term to terrain radiation.

For point calculations, a large variety of empirical functions have been developed to relate global radiation to climatic and topographic variables without explicitly differentiating between direct and diffuse radiation. Based on measurements in the Alps, Sauberer (1955) proposed a parameterization for global radiation. Wagner (1980a) presents scattergrams for daily sums of global radiation in the Alps depending on the month and assuming mean daily cloudiness. Kasten (1983) computed global radiation as a function of top of atmosphere radiation, optical air mass and turbidity, deriving the latter two from zenith angle, elevation, air temperature and humidity. Based on Kasten (1983), Konzelmann *et al.* (1994) derived a parameterization for global radiation using air temperature, vapour pressure, albedo, cloud amount and elevation at the ETH camp on West Greenland.

On a larger scale, numerous distributed radiation models have been developed to compute global radiation for each grid element of an elevation model. Munro and Young (1982) and Varley and Beven (1996) proposed global radiation models for steep terrain treating direct and diffuse radiation separately. Dozier (1980) developed a highly sophisticated spectral model for clear-sky solar radiation, incorporating separate transmission functions for various absorption

and scattering processes as a function of wavelength and explicitly accounting for the interactions with the snow surface and surrounding terrain. Models of this type are complicated and require estimates of various atmospheric attenuation parameters and of the ozone and water vapour distribution with altitude as input, which are often unknown.

In some distributed melt models, this problem is circumvented by including measured global radiation into model formulations, thus scaling calculations to measurements (e.g., Arnold *et al.*, 1996). Spatial variations due to topographic effects are considerably more pronounced for the direct than the diffuse component. Hence, in distributed modelling measured global radiation needs to be split into direct and diffuse components prior to extrapolation. Hock and Holmgren (2005) accomplished this by adapting an empirical relationship between the ratio of diffuse radiation to global radiation and the ratio of global radiation to top of atmosphere radiation as suggested by Collares-Pereira and Rabl (1979). Following Ohta (1994) direct solar radiation thus obtained I_s divided by potential clear-sky direct radiation at the weather station I_{cs} was then used to compute direct radiation for each grid cell I:

$$I = \frac{I_s}{I_{sc}} I_c \qquad (10)$$

where I_c is potential clear-sky direct radiation for the grid cell to be calculated (see equation 4). The ratio I_s/I_{cs} which is assumed constant in space accounts for the deviations from clear-sky conditions and tends to decrease with increasing cloudiness. Escher-Vetter (2000) and Hock and Noetzli (1997) extrapolated global radiation without explicit separation into the direct and diffuse components by multiplying the ratio of measured global radiation to I_{cs} by I_c to obtain global radiation for each grid cell. Both methods can only be applied if the grid cell to be computed and the measuring site are not topographically shaded.

3 Albedo

Warren (1982) gives a comprehensive review of snow albedo. Albedo, generally defined as the averaged reflectivity over the spectrum from 0.35 to 2.8 μm, varies considerably on glaciers, both in space and time. Ranging from 0.1 for dirty ice to more than 0.9 for fresh snow it controls the spatial and temporal distribution of meltwater production to a large extent, thus rendering albedo a key parameter in glacier melt simulations. Summer snowfall events can reduce melt and runoff considerably because of abruptly enhanced albedo. Snow albedo displays considerable short-term fluctuations. Fresh-snow albedo may drop by 0.3 within a few days due to metamorphism. Temporal variations of ice albedo are small compared to those of snow (Cutler and Munro, 1996; Brock *et al.*, 2000a; Jonsell *et al.*, 2003). However, small-scale spatial albedo variations may occur on glacier ice and cause large spatial differences in ablation (van de Wal *et al.*, 1992; Konzelmann and Braithwaite, 1995). Glacier albedo often is considerably modified by deposits of sediment or rock debris.

Albedo is determined by factors related to the surface itself, such as grain size, water content, impurity content, surface roughness, crystal orientation and structure, and by factors related to the incident shortwave radiation, such as the wavelength or whether the sunlight is diffuse or direct. Water in interstices between grains indirectly affects albedo by increasing grain size which in turn reduces albedo. Surface albedo increases with increasing cloudiness and atmospheric water content. Clouds preferentially absorb near-infrared radiation, thus increasing the fraction of visible light, for which albedo is higher (Marshall and Warren, 1987). This effect is enhanced by multiple reflection between cloud base and the glacier surface. Snow albedos have been found to increase by 3–15% when moving from clear-sky to overcast conditions (Holmgren, 1971; Greuell and Oerlemans, 1987). Jonsell *et al.* (2003) report short-term albedo variations over snow by

>0.1 due to cloud fluctuations while the response of albedo over ice to varying cloudiness was considerably smaller. Albedo is highest at low angles of incidence as a result of the Mie scattering properties of ice and snow grains dominating other effects such as the spectral change in global radiation.

Modelling albedo is complicated, as it is exceedingly difficult to quantitatively relate albedo variations to their causes. Opposing factors may influence the local conditions in different ways. On glaciers, snow and ice albedo must be treated separately due to their substantial difference and different temporal variability. Radiative transfer modelling studies indicate that snow albedo is primarily explained by the snow grain size. Models accounting for the effects of grain size as well as atmospheric controls have been proposed by Warren and Wiscombe (1980), Choudhury and Chang (1981), Marshall and Warren (1987) and Marks and Dozier (1992). However, due to large data requirements, they are generally not applicable for operational purposes and surrogate methods are used instead. A common surrogate method is the so-called aging curve approach, which calculates the decreasing snow albedo as a function of time after the last significant snowfall. The formulation of the Corps of Engineers (1956) has been widely used:

$$\alpha = \alpha_0 + b e^{-n_d k} \qquad (11)$$

where α_0 is the minimum snow albedo, n_d the number of days since the last significant snowfall and b and k are coefficients. Kuzmin (1961) presented nomogramms for the decay of snow albedo for different snow depths. A large variety of snow albedo parameterizations have been proposed incorporating one or more variables such as snow depth, snow density, melt rate, sun altitude, air temperature and accumulated daily maximum air temperatures since the last snowfall (e.g., Brock *et al.*, 2000a; Willis *et al.*, 2002 – see summary in Brock *et al.*, 2000a). Although these generally generate satisfactory albedo simulations for the site developed and calibrated, they need further independent testing to promote confidence in their general applicability.

In contrast to snow albedo, very few studies have focused on ice albedo (e.g., Cutler and Munro, 1996; Brock *et al.*, 2000a). Ice albedo is often treated as a temporal and spatial constant (Konzelmann and Braithwaite, 1995; Hock and Noetzli, 1997), albedo jumping from a fixed or variable snow value to a lower fixed ice value as soon as all snow has melted. Oerlemans (1992) proposed an energy-balance model including modelling of glacier albedo. His albedo parameterization is based on the assumption of a downglacier decrease in albedo owing to an increase in concentrations of dust and debris. He defines a 'background albedo profile' as a function of the elevation relative to the equilibrium line at the end of the ablation season and various empirically determined constants. Snow albedo is superimposed on this profile as a function of snow depth. Arnold *et al.* (1996) slightly modified this approach by considering fresh snow separately.

4 Longwave radiation

Longwave incoming radiation is emitted mostly by atmospheric water vapour, carbon dioxide and ozone. Variations are largely due to variations in cloudiness and in the amount and temperature of the water vapour. Due to the latter, longwave irradiance tends to decrease with altitude. Although downward radiation is emitted from all levels of the atmosphere, the largest portion reaching the surface originates from the lowest layers. Irradiance can be modelled using radiative transfer equations, requiring input of temperature and water vapour profiles and the distribution of the concentrations of CO_2 and O_3. A review of models is given by Ellingston *et al.* (1991). In melt models, longwave irradiance is usually estimated from empirical relationships based on standard meteorological measurements exploiting the fact that longwave irradiance correlates well with air temperature and vapour pressure at screen level, usually at 2 m above the surface

(Kondratyev, 1969). Over melting snow and ice surfaces, however, the use of screen-level temperature may underestimate longwave irradiance due to the proximity of the melting surface which restricts temperature increase of the lowest air layers (van den Broeke, 1996). Generally, the equations for longwave irradiance $L\downarrow$ take the form:

$$L\downarrow = \epsilon_c \sigma T_a^4 F(n) \tag{12}$$

where ϵ_c is the full-spectrum clear-sky emissivity, σ is the Stefan-Boltzmann constant (5.67×10^{-8} W m^{-2} K^{-4}), T_a is air temperature (K) and $F(n)$ is a cloud factor describing the increase in radiation due to clouds as a function of cloud amount n. Effective or apparent emissivity ϵ_e defined by the product of ϵ_c and $F(n)$ ranges from approximately 0.7 under clear-sky conditions to close to unity under overcast conditions. A variety of parameterizations have been suggested to relate clear-sky emissivity to screen-level measurements of air temperature and humidity. Widely quoted expressions are those of Ångström (1916):

$$\epsilon_c = A - B \cdot 10^{-C\rho} \tag{13}$$

and Brunt (1932):

$$\epsilon_c = a + b\sqrt{e_a} \tag{14}$$

where A, B, C, $a = 0.51$ and $b = 0.066$ are empirically determined coefficients, ρ is absolute humidity and e_a is vapour pressure [hPa]. The coefficients obtained by different authors are very variable, as is to be expected since they vary with the time of year and location. These equations do not work on subdaily timescales. Wagner (1980b) found good results on Hintereisferner using Brunt's and Ångström's formulae, although Brunt's formula tended to yield 7–8% lower values than Ångström's expression. A more physically based approach has been developed by Brutsaert (1975) with the advantage that it does not require calibration to local conditions. It is based on the integration of the Schwarzschild's transfer equations for simple atmospheric profiles of temperature [K] and

vapour pressure [hPa], but neglects greenhouse gases other than water vapour:

$$\epsilon_c = 1.24(e_a/T_a)^{1/7} \tag{15}$$

Over glaciers, Braithwaite and Olesen (1990b) and Arnold *et al*. (1996) applied the expression for effective emissivity ϵ_e suggested by Ohmura (1981), which includes the effect of clouds:

$$\epsilon_e = 8.733 \times 10^{-3} T_a^{0.788}(1 + kn) \tag{16}$$

where T_a is air temperature [K], thus accounting for the increase in absolute humidity with temperature, and n is the cloud amount. The coefficient k is a function of cloud type, for which Ohmura (1981) listed eight values corresponding to different cloud types. Konzelmann *et al*. (1994) derived parameterizations for hourly and daily longwave irradiance at the ETH camp in Greenland. The hourly formulation for effective emissivity is:

$$\epsilon_e = \epsilon_c(1 - n^p) + \epsilon_{oc}n^p \tag{17}$$

Clear-sky emissivity ϵ_c as obtained from measured longwave radiation under clear-sky conditions ($\epsilon_c = L\downarrow/\sigma T_a^4$) was related to measured e/T to fit a modified version of Brutsaert's (1975) equation, yielding $\epsilon_c = 0.23 + 0.484(e_a/T_a)^{1/8}$ with e_a in Pa. By considering greenhouse gases other than water vapour (ϵ_c is different from zero (0.23) in a completely dry atmosphere), this formulation was superior to the original one by Brutsaert (1975). The emissivity of a completely overcast sky $\epsilon_{oc} = 0.952$ and the coefficient $p = 4$ were obtained empirically from observations of $L\downarrow$, T_a, e_a and cloud amount. Although the high power ($p = 4$) resulted from the site-specific cloud climatology, where high cloudiness was primarily caused by low clouds and low cloudiness by high clouds, the expression has been used at other sites in Greenland (e.g., Greuell and Konzelmann, 1994; Zuo and Oerlemans, 1996) and in the Alps (Plüss, 1997). Coefficients were adjusted to the conditions on Pasterzegletscher by Greuell *et al*. (1997)

and used on Moteratschgletscher by Oerlemans (2000). At a low-elevation site in Greenland, van den Broeke (1996) obtained considerable underestimation of longwave irradiance using equation 17. The same was true when the formula derived in polar regions by Koenig-Langlo and Augstein (1994) was applied. Van den Broeke (1996) attributes the underestimation to a stronger surface inversion than at the Greenland ETH camp for which the coefficients were determined. In general, satisfactory results can be achieved with such parameterization, however, it is necessary to adjust coefficients for different sites.

In mountainous areas, surrounding topography can cause significant spatial variations in longwave irradiance. This is neglected in many distributed energy-balance models, which assume longwave irradiance is spatially uniform. Longwave sky irradiance is reduced by obstructed sky due to surrounding terrain. Conversely, the surface receives additional radiation from the surrounding terrain and the air between the terrain and the receiving surface. The importance of terrain contributions to the incoming longwave radiation has been pointed out by Olyphant (1986). Plüss and Ohmura (1997) found variations between 160 and 240 W m^{-2} in longwave incoming radiation $L\downarrow$ on a clear day in a high alpine area, solely due to topographic influence. Marks and Dozier (1979) considered topographic modification of longwave irradiance by:

$$L\downarrow = (\epsilon_a \sigma T_a^4)V_f + (\epsilon_s \sigma T_s^4)(1-V_f) \quad (18)$$

where ϵ_a and ϵ_s are emissivities of the air and the surrounding surface, respectively, T_a and T_s are the temperature of the air and the surface, respectively, and V_f is the thermal view factor, related to the unobscured fraction of the hemisphere (see equations 7 and 8). The first term represents sky irradiance and the second term refers to terrain irradiance. The effect of the air between the emitting surface and the receiving surface was neglected. Based on calculations with a spectral

radiation transfer model (LOWTRAN7), Plüss and Ohmura (1997) revealed that neglecting this effect may lead to significant underestimation of irradiance, especially if the air temperature exceeds the snow surface temperature, which is typical of melting surfaces. They derive a simple parameterization for longwave irradiance in completely snow-covered mountainous terrain accounting for this effect. Despite the large anisotropy in longwave irradiance under clear-sky conditions (Kondratyev, 1969), Plüss and Ohmura (1997) showed that the assumption of isotropy produced only small errors in all investigated cases. Under cloudy conditions, longwave irradiance is nearly isotropic.

Longwave outgoing radiation $L\uparrow$, referring to the radiation emitted by and reflected from the surface, can be calculated from:

$$L\uparrow = \epsilon_s \sigma T_s^4 + (1-\epsilon_s)L\downarrow \quad (19)$$

with ϵ_s the emissivity of the snow cover. In many computations the snow and ice surfaces are assumed to be at melting point. Combined with an assumed emissivity of unity, the corresponding longwave emission amounts to 315.6 W m^{-2}.

5 Turbulent heat fluxes

The turbulent fluxes of sensible and latent heat are driven by the temperature and moisture gradients between the air and the surface and by turbulence in the lower atmosphere as the mechanism of vertical air exchange. These fluxes are generally small when averaged over periods of weeks or months and compared to the net radiation flux (Table 2; Willis *et al.*, 2002), but they can exceed the radiation fluxes over short time intervals of hours and days, and in mid-latitude maritime environments also over longer periods (e.g., Hogg *et al.*, 1982; Marcus *et al.*, 1984). Highest melt rates often coincide with high values of the turbulent fluxes (Hay and Fitzharris, 1988). The latent heat flux is of major importance for the short-term variations of melt rates on temperate glaciers (Lang, 1981). Sublimation is

important at high altitudes and high latitudes, such as the blue-ice areas of the Antarctic ice sheet where all ablation occurs by sublimation (Bintanja, 1999). A review of turbulent heat transfer over snow and ice is given by Morris (1989).

The turbulent heat fluxes can be measured directly by eddy-correlation techniques. These require sophisticated instrumentation with continuous maintenance, which render them unsuitable for operational purposes. Consequently, such studies are rare and restricted to short periods of time (e.g., Munro, 1989; Forrer and Rotach, 1997; van der Avoird and Duynkerke, 1999). Therefore, the turbulent heat fluxes are often described by gradient-flux relations. These are based on the theoretical work of Prandtl (1934) and Lettau (1939) and they were first introduced to snow and ice by Sverdrup (1936). In the surface layer, the relations are based on the assumption of constant fluxes with height and horizontal, homogeneous conditions. Accordingly, the turbulent energy fluxes of sensible heat Q_H and of latent heat Q_E are proportional to the time-averaged gradients of potential temperature $\bar{\theta}$ and specific humidity $\bar{q}$ in the surface boundary layer and can be expressed by:

$$Q_H = \rho_a c_P \, K_H \frac{\partial \bar{\theta}}{\partial z} \qquad (20)$$

$$Q_E = \rho_a L_v \, K_E \frac{\partial \bar{q}}{\partial z} \qquad (21)$$

where ρ_a is the air density, c_P is the specific heat capacity of air, L_v is the latent heat of evaporation, z is the height above the surface, K_H and K_E are the eddy diffusivities for heat and vapour exchange, respectively. K_H and K_L specify the effectiveness of the transfer process and depend on wind speed, surface roughness and atmospheric stability.

The profile method involves measurements of $\bar{\theta}$, $\bar{q}$ and wind speed $\bar{u}$ at preferably more than two levels within the first few metres above the surface (e.g., de la Casinière, 1974; Forrer and Rotach, 1997).

The method has the disadvantage of large sensitivity to instrumental errors, especially if only two levels of measurements are employed. Because detailed profile measurements are seldom available, the so-called bulk aerodynamic method has frequently been applied for practical purposes (e.g., Braithwaite *et al.*, 1998; Oerlemans, 2000). It exploits the fact that the surface conditions of a melting surface are well defined (T = 0°C, e = 6.11 hPa), thus allowing for the computation of the sensible Q_H and the latent heat flux Q_E from only one level of measurements. Integrating equations 20 and 21, the bulk aerodynamic expressions read:

$$Q_H = \rho_a c_P \, C_H \, \bar{u} \, (\bar{\theta}_z - \bar{\theta}_s) \qquad (22)$$

$$Q_E = \rho_a L_v \, C_E \, \bar{u} \, (\bar{q}_z - \bar{q}_s) \qquad (23)$$

where $\bar{u}$ is mean wind speed, $\bar{\theta}_z$ and $\bar{\theta}_s$ are mean potential temperatures and $\bar{q}_z$ and $\bar{q}_s$ are mean specific humidities at height z and the surface, respectively. In practice, the specific humidity term $(\bar{q}_z - \bar{q}_s)$ is often replaced by $(0.622/p)(\bar{e}_z - \bar{e}_0)$ with p the atmospheric pressure and $\bar{e}$ the mean vapour pressure. The exchange coefficients for heat C_H and vapour pressure C_E are given by:

$$C_H = \frac{k^2}{[\ln(z/z_0) - \psi_M(z/L)]\,[\ln(z/z_{0T}) - \psi_H(z/L)]} \qquad (24)$$

$$C_E = \frac{k^2}{[\ln(z/z_0) - \psi_M(z/L)]\,[\ln(z/z_{0E}) - \psi_E(z/L)]} \qquad (25)$$

where $k = 0.4$ is the von Kármán constant, Ψ is the integrated form of the Monin-Obukhov stability functions ϕ as an atmospheric stability correction, the subscripts M, H and L refering to momentum, heat and water vapour, respectively. Under neutral conditions the functions Ψ assume a value of zero. The roughness length for wind z_0, defined as the height above the surface where $\bar{u} = 0$, is related in a complex way to the roughness of

the surface. The roughness lengths for temperature z_{0T} and vapour pressure z_{0e} are scaling parameters lacking a well-defined physical meaning. The stability functions Ψ depend on the stability parameter z/L, where L denotes the Monin-Obukhov-length, which in the stable boundary layer can be interpretated as the height at which the rate of turbulent energy production by shear stress balances the energy consumption by buoyancy forces (Obukhov, 1946). The quantity z/L, in turn, depends on Q_H among other factors, thus an iterative loop is required to compute the turbulent fluxes (e.g., Munro, 1989). The exchange coefficient is often also referred to as the transfer or drag coefficient. However, direct comparison of numerical values between studies is often difficult because the number and type of parameters and coefficients lumped into these numerical values vary among authors. For example, Moore (1983) and Price and Dunne (1976) lump the wind speed into the exchange coefficient expressions (equations 24 and 25).

A variety of empirical expressions have been proposed to define the form of the stability functions (Högström, 1988). A frequently used approximation is $\alpha\, z/L$ where $\alpha = 5$ for stable stratification (Dyer, 1974). Forrer and Rotach (1997) showed that for large stability ($z/L > 0.4$) the linear form of the stability functions was not appropriate at a site on the Greenland ice sheet, but the nonlinear expressions suggested by Beljaars and Holtslag (1991) yielded better results. Due to its simplicity, a commonly used stability criterion is the Richardson number, which in its bulk form is defined by:

$$R_b = \frac{g}{T_z} \frac{(T_z - T_s)(z - z_0)}{u_z^2} \qquad (26)$$

where g is the acceleration of gravity and T_z and T_s are absolute temperatures at height z and the surface, respectively. For stable stratification ($R_b > 0$), which prevails over melting glaciers, one way to relate the Richardson

number to the stability function is given by Webb (1970) where the exchange coefficient C for the property x to be transported reads:

$$C_x = \frac{k^2}{\ln(z/z_0)\ln(z/z_{0x})}(1 - 5.2R_b)^2 \quad (27)$$

The magnitude of correction either by the Monin-Obukhov stability or by the Richardson number increases considerably as the wind speed decreases.

Although the bulk aerodynamic approach is very convenient due to its simplicity, much uncertainty about its application to glacier surfaces remains. One problem concerns the specification of roughness lengths. They can be derived from detailed measurements of wind, temperature and humidity profiles. However, these are seldom available and the roughness lengths are often estimated from published data (e.g., Greuell and Oerlemans, 1989; Konzelmann and Braithwaite, 1995). This poses a problem because the roughness lengths for wind reported over snow and ice vary by several orders of magnitude (summaries in Moore, 1983; Braithwaite, 1995a) ranging from 0.004 mm (Inoue, 1989) to 70 mm (Jackson and Carroll, 1978) over snow and from 0.003 mm (Antarctic blue ice area; Bintanja and van den Broeke, 1995) to 120 mm (van den Broeke, 1996) over glacier ice. Generally, z_0-values of a few mm tend to be assumed in glacier applications. Changes in z_0 and z_{0T} by one order of magnitude can result in differences in the turbulent heat fluxes by a factor of two (Munro, 1989; Hock and Holmgren, 1996) demonstrating the significance of accurate roughness length determination.

The relationship between the roughness lengths of wind, heat and vapour pressure is another matter of discussion. The principle of similarity is often invoked (e.g., Streten and Wendler, 1968; Hay and Fitzharris, 1988; Brun *et al.*, 1989; Munro, 1989; Zuo and Oerlemans, 1996), although there is evidence that the surface roughnesses for heat and vapour pressure are smaller than z_0 by one or

two orders of magnitude (Sverdrup, 1935; Holmgren, 1971; Ambach, 1986; Beljaars and Holtslag, 1991; Smeets *et al.*, 1998). Conversely, Morris *et al.* (1994) concluded the opposite from energy-balance modelling, namely that z_{0T} and z_{0E} were considerably larger than the aerodynamic roughness lengths. Data analysis from Greenland gave values for z_T of about 10 to 100 times larger than z_0 (Calanca, 2001). Braithwaite (1995a) suggests that the assumption of unequal roughness lengths is not strictly necessary, because an 'effective roughness length' satisfying $z_0 = z_{0T} = z_{0E}$ can be chosen so that the exchange coefficient gives the same value when applying equations 24 and 25. The roughness length of vapour pressure is generally assumed to be equal to the one for heat. However, very few studies, exist due to the inherent difficulty of accurately measuring vapour pressure profiles over glaciers. In addition, roughness lengths will vary in space and time (Plüss and Mazzoni, 1994; Greuell and Konzelmann, 1994; Calanca, 2001). Holmgren (1971) observed an increase in roughness lengths with decreasing wind speed; Anderson (1976) a decrease with time during the snow melt season.

Alternative approaches to estimating roughness lengths have been suggested by Lettau (1969) who calculated them from the height and cross-sectional area of surface forms, and by Andreas (1987) who used surface renewal theories and expressed z_{0T}/z_0 and z_{0E}/z_0 as functions of the roughness Reynolds number. In a study on Greenland, van den Broeke (1996) obtained $z_0 = 0.8$ mm from wind profiles, but at the same location $z_0 = 120$ mm from the microtopographical survey according to Lettau (1969), clearly showing the difficulties involved in obtaining accurate estimates of roughness lengths. The latter value yielded more realistic results for the energy balance. Herzfeld *et al.*, (2000) designed a sensor recording variations in microtopography at 0.2 m $\times$ 0.1 m resolution when pulled across the ice surface. The data are analysed using geostatistical methods.

More studies are needed to evaluate the method in terms of suitability for use in turbulent flux calculations. Because of the difficulties involved in specifying transfer coefficients or roughness lengths, some authors treat them as residuals in the energy-balance equation (e.g., La Chapelle, 1961; Braithwaite *et al.*, 1998; Zuo and Oerlemans, 1996; Oerlemans, 2000). Sufficient accuracy can only be obtained over longer periods of time. A unique attempt to incorparate spatial and temporal variations in z_0 into a distributed energy-balance model has been made by on Haut Glacier d'Arolla (Brock *et al.*, 2000b). Over snow, z_0 was parameterized as a function of accumulated daily maximum temperatures since the last snowfall, to account for increasing snow roughness during snowmelt. However, no relationship could explain the observed variation over ice, when relating z_0 derived from the formula of Lettau (1969) to various meteorological variables. The parameterization over snow needs further testing at other sites.

Many energy-balance models applied to snow and ice do not include a formal stability correction in the bulk approach (e.g., Föhn, 1973; Hogg *et al.*, 1982; Konzelmann and Braithwaite, 1995; Oerlemans, 2000), thus assuming logarithmic wind profiles despite prevailing stable stratification. Braithwaite (1995a) points out that the uncertainty in surface roughness may cause larger errors than neglecting stability. Some authors identify a tendency of energy-balance modelling to underestimate glacier melt and attribute this error to an underestimation of the turbulent fluxes (e.g., Harding *et al.*, 1989; Konzelmann and Braithwaite, 1995; van den Broeke, 1996). Brun *et al.* (1989) concluded that, under light wind conditions, energy gain at the surface by heat conduction through the air and by vapour diffusion due to vapour gradients in the air may be higher than by turbulent transfer. In order to obtain larger fluxes, they modified equations 22 and 23 in their snow model by replacing the wind speed u by the empirical relation $a + b \cdot u$, where

a and *b* are experimentally determined. King and Anderson (1994) and Martin and Lejeune (1998) showed that turbulent heat fluxes are sensitive to orography and concluded that exchange coefficients in complex topography must be increased. Martin and Lejeune (1998) proposed an empirical parameterization which reduces the Richardson number under stable atmospheric conditions, thus allowing for turbulent heat transfer even with strong stability. However, they emphasize that parameterization of the turbulent fluxes is highly dependent on the site, and that a universal or simple formula can not be determined. De la Casinière (1974) and Halberstam and Schieldge (1981) observed temperature profile anomalies that would lead to serious errors in an estimate of the turbulent heat fluxes if the data at standard height (2 m) were used. Due to radiative heating of the air above the surface, the temperature maxima occurred within the first couple of decimetres above the surface, thus violating the assumption of constant fluxes with height. Munro and Davies (1972) gave an upper limit of 1 m for the surface boundary layer thickness. Contrary to theory, Grainger and Lister (1966) showed that the logarithmic wind profile is valid over a wide range of stability, and on Greenland, Forrer and Rotach (1997) found no tendency for the stability function for heat to increase with increasing atmospheric stability, although they lack an explanation in terms of boundary layer theory.

Experimental and theoretical evidence is mounting that Monin-Obukhov theory, on which both profile and bulk methods are based, is not applicable over a sloping glacier surface due to violation of assumptions such as homogeneous, infinite, flat terrain and constant flux with height (Holmgren, 1971; Denby and Greuell, 2000). The turbulent scaling laws used in the theory are altered by the wind-speed maximum. By observations and second-order modelling, Denby and Greuell (2000) showed that profile methods will severely understimate turbulent fluxes when a wind-speed maximum is present, but

found that the bulk method was appropriate at least in the region below the wind-speed maximum despite large scatter in the data.

The discussion above reveals that large uncertainty remains in the determination of turbulent fluxes over glaciers, in terms of the suitability of bulk and profile methods, the determination of exchange coefficients or roughness lengths and their spatial and temporal variability, and the application of stability corrections. Further research is needed to explore and develop alternative new methods that are more suitable over sloping glacier surfaces subject to glacier winds. More eddy correlation measurements are needed on valley glaciers. In glaciology such studies have been conducted over ice sheets, while to date only one reported study concerns a valley glacier (Smeets *et al.*, 1998).

6 Ice heat flux

Before surface melting can occur, the temperature of the ice/snow surface must be raised to 0°C. The energy necessary to heat a cold snow or ice mass to 0°C defines the cold content given by

$$C = -\int_0^z \rho(z) c_P \, T(z) \mathrm{d}z \qquad (28)$$

where ρ is the snow or ice density, c_P is the specific heat of snow or ice, T is the temperature at depth z (°C) and Z is the maximum depth of subfreezing temperatures. The cold content of both winter snow cover and the surface ice layers can be an important retention component, significantly contributing to the delay between surface melt and melt-derived streamflow (e.g., Kattelmann and Yang-Daqing, 1992). Closely connected to the cold content is the formation of super-imposed ice (König *et al.*, 2002) and internal accumulation (Trabant and Mayo, 1985; Schneider and Jansson, 2004). The former forms when water percolating through the snow layer refreezes at the impermeable cold ice surface, while the latter refers to water refreezing in the firn area, below the last summer surface. These processes can be

crucial for glacier mass balance, especially in polar regions, and for correct calculations of equilibrium line altitude. The energy balance is also affected, as the albedo and surface roughness are modified.

a Ice: Near-surface glacier ice is warmed up primarily by heat conduction and by absorption of penetrating shortwave-radiation. For temperate glacier ice, the heat flux is zero except during occasional nocturnal freezing. For cold glacier ice or glaciers with a perennial cold surface layer, heat flux into the ice can be a substantial energy sink. At a site in North Greenland, 11% of the total energy surplus at the surface was used to heat up the ice, and thus was not available for melt (Konzelmann and Braithwaite, 1995). Heat flux across the ice surface is given by:

$$Q_G = \int_0^z \rho c_p \frac{\partial T}{\partial t} \mathrm{d}z \qquad (29)$$

with $\partial T/\partial t$ the rate of change of ice temperature. This flux can be estimated from temperature-depth profiles down to the base of the seasonally affected layer, usually 10–15 m below the surface (Paterson, 1994). The heat flux is then computed from the change in cold content with time. Konzelmann and Braithwaite (1995) propose a method to compute the ice heat flux when temperature measurements are shallower than the depth of seasonal temperature fluctuations; however, the temperature changes with time are assumed constant. Then the heat flux through the glacier surface is calculated as the intercept in a regression equation of the heat flux at depth z versus depth, where the englacial heat flux is calculated from ice temperature gradients and thermal conductivity. Greuell and Oerlemans (1987) model the temperature profile inside the glacier down to a depth of ~25 m, considering conduction and advection of snow/ice normal to the surface and energy release or consumption by phase changes. Results showed that ablation is considerably overestimated at higher elevations if glacier temperatures were kept at 0°C, thus emphasizing the need to consider the occurrence of subfreezing glacier temperatures in models.

b Snow: Quantitative assessment of the energy transfer within a cold snowpack is more difficult due to a complex interplay of hydrology and heat transfer (Colbeck, 1972). The mechanisms of heat transfer in snow are governed by penetration of shortwave radiation, internal movement of water/water vapour and phase changes. The most efficient process for snowpack warming is the release of latent heat by refreezing of percolating melt or rain water. Physical-based snow models accounting explicitly for heat and mass transfer within a snow cover, including simulation of the evolution of temperature, density, water content, metamorphism and snow stratigraphy, have been suggested by several authors (e.g., Anderson, 1976); those few which have been converted into fully developed computer programs and widely tested include CROCUS (Brun *et al.*, 1989), SNTHERM (Jordan, 1991) and DAISY (Bader and Weilenmann, 1992).

More conceptual approaches have been developed in order to circumvent excessive data requirements. Van de Wal and Russel (1994) developed an algorithm where energy deficits from previous time steps were compensated before allowing melt. This approach was extended by adjusting iteratively the surface temperature until the trial ablation for the time step becomes zero in case negative melt was computed (Escher-Vetter, 1985b; Braithwaite *et al.*, 1998; Hock and Holmgren, 2005). An iterative procedure is necessary because surface temperature also affects outgoing longwave radiation, the turbulent heat fluxes and the heat flux supplied by rain. A common way to consider the cold content of snow in conceptual melt models is to use the concept of 'negative melt' (e.g., Braun and Aellen, 1990). The amount of refreezing water is computed from air temperature and a factor of refreezing in case computed melt turns negative.

7 Other heat fluxes

The sensible heat flux of rain is generally unimportant in the overall surface energy balance of a glacier, and is thus neglected in many models. A rainfall event of 10 mm at 10°C on a melting surface would produce a heat flux of 2.4 W m^{-2} averaged over a day, hence negligible compared to other heat fluxes. Precipitation may be a significant short-term heat source only when precipitation is heavy, prolonged and warm, as encountered in maritime areas exposed to storms originating over warm oceans. One day on Ivory Glacier, New Zealand, the heat flux by rain contributed 37% of the daily ablation of 6.2 mm (Hay and Fitzharris, 1988). The heat flux by rain Q_R is given by:

$$Q_R = \rho_w c_w \, R(T_r - T_s) \qquad (30)$$

where ρ_w is the density of water, c_w is the specific heat of water (4.2 kJ kg^{-1} K^{-1}), R is the rainfall rate and T_r and T_s are the temperatures of rain and the surface, respectively. Although energetically of minor importance, rain may affect melt indirectly by increasing the liquid water content of a glacier surface and thus reducing its albedo.

On alpine glaciers, advection of warm air from adjacent valley slopes and moraines may contribute substantially to glacier melt (Wendler, 1975). This advective heat flux is not considered in the vertical flux equation used in the one-dimensional energy-balance models generally applied in melt modelling. For alpine tundra environments, modelling studies have demonstrated that local advection of heat from snow-free patches considerably enhances snow melt rates along the leading edges of snow-covered patches (Olyphant and Isard, 1988; Marsh and Pomeroy, 1997; Essery, 1999).

Moore (1991) investigated the possibility of sensible heat being advected by supraglacial runoff. Through numerical modelling, he concluded that such advection will be negligible on a macroscale under most conditions, but may cause microscale variations in ice melt.

III Temperature-index melt models

Temperature-index models or degree-day models assume an empirical relationship between melt and air temperature based on a strong and frequently observed correlation between these quantities. A detailed review of the method and recent advances in distributed temperature-index modelling is given by Hock (2003). Since air temperature is usually the most readily available data quantity and is reasonably easy to extrapolate and forecast, temperature-index models have been the most widely used method of ice and snow melt computations. Applications are widespread and include the prediction of melt for operational flood forecasting and hydrological modelling (WMO, 1986), glacier mass balance modelling (e.g., Laumann and Reeh, 1993; Oerlemans *et al.*, 1998) and assessment of the response of snow and ice to predicted climate change (e.g., Braithwaite and Zhang, 1999). Most operational runoff models, e.g., HBV model (Bergström, 1976), SRM model (Martinec and Rango, 1986), UBC model (Quick and Pipes, 1977), HYMET model (Tangborn, 1984) and even versions of the physically based SHE model (Bøggild *et al.*, 1999), apply temperature-index methods for melt modelling.

Although the concept involves a simplification of complex processes that are more properly described by the surface energy balance, temperature-index models often match the performance of energy-balance models on a catchment scale (WMO, 1986; Rango and Martinec, 1995). The success of the temperature-index method is generally attributed to the high correlation of temperature with various components of the energy-balance equation. Longwave incoming radiation and the turbulent heat fluxes depend strongly on temperature, and temperature in turn is affected by global radiation, although not in a simple way (Kuhn, 1993; Ohmura, 2001).

The classical degree-day model relates ice or snow melt, M [mm], during a period of n time intervals, Δt, to the sum of positive

air temperatures of each time interval, T^+, during the same period:

$$\sum_{i=1}^{n} M = DDF \sum_{i=1}^{n} T^+ \cdot \Delta t \qquad (31)$$

The factor of proportionality is the *degree-day factor*, *DDF*, expressed in mm d^{-1}K^{-1} for Δt expressed in days and temperature in °C (Braithwaite, 1995b; Hock, 2003).

   Degree-day factors vary considerably in space and time because they implicitly account for all terms of the energy budget, which vary in relative importance. High relative contributions of sensible heat flux to the heat of melt favour low degree-day factors (Ambach, 1988). On average, reported values for different sites based on melt measurements range from 2.5 to 11.6 mm d^{-1}K^{-1} and 6.6 to 20.0 mm d^{-1}K^{-1} for snow and ice, respectively (see summary in Hock, 2003). Degree-day factors for ice generally exceed those for snow, due to lower albedo of ice compared to that of snow. In addition, enormous small-scale spatial variability occurs partially due to topographic effects. On Storglaciären (3 km^2) hourly degree-day factors computed from melt determined from a distributed energy-balance model on a 30 m resolution grid ranged from 0 to 16 mm d^{-1}K^{-1} for the same hour of the day (Hock, 1999). Seasonal variations in the DDF can be expected due to the seasonal variation in clear-sky direct radiation, and in the case of snow, due to snow metamorphism, which generally decreases snow albedo, thus increasing the DDF, as the melt season progresses (Kuusisto, 1980). Measurements (Singh and Kumar, 1996) and modelling studies (Hock, 1999) indicate large diurnal variations in degree-day factors (0 to >15 mm d^{-1}K^{-1}) caused by diurnal radiation fluctuations, implying that constant melt factors are inadequate for subdaily (e.g., hourly) melt computations.

   Many temperature-index based runoff models consider seasonal variations in melt factors. For instance, the UBC runoff model (Quick and Pipes, 1977) uses a monthly variable melt factor, while the HBV-ETH model (Braun *et al.*, 1993) determines the melt factor from sinusoidal interpolation between a minimum value on 21 December and a maximum value on 21 June. Schreider *et al.* (1997) and Arendt and Sharp (1999) varied the degree-day factor according to albedo.

   Because degree-day factors are influenced by all components of the energy balance, many attempts have been made to strengthen the physical foundation of the method by incorporating more variables, such as wind speed, vapour pressure or radiation (e.g., Willis *et al.*, 1993). There is a gradual transition from simple degree-day approaches to energy-balance type expressions by increasing the number of input variables in melt computations. The widely quoted combination method by Anderson (1973) applies a simple degree-day approach during dry periods and a simplified empirical energy-balance formulation during rainy periods. The UBC runoff model (Quick and Pipes, 1977) and the HYMET runoff model (Tangborn, 1984) include the daily temperature range in addition to air temperature itself as climatic input to their melt routines. Various studies have added a radiation term, often in form of shortwave or net radiation balance (Martinec, 1989; Kustas and Rango, 1994; Kane and Gieck, 1997), thus achieving better results on a daily or hourly basis compared to the classical degree-day method.

   To account for spatial variability in melt rates, while employing spatially constant degree-day factors, melt-runoff models often divide the basin into elevation bands to consider a decrease in melt with increasing elevation, or also into aspect classes to account for enhanced melt on south-facing slopes compared to north-facing slopes (Braun *et al.*, 1994). In recent years, such approaches have been considerably advanced by explicitly varying the degree-day factor for each slope/aspect class (Brubaker *et al.*, 1996; Dunn and Colohan, 1999) or for each grid

element of a digital elevation model in a fully distributed manner. Daly *et al.* (2000) increase the melt factor for each grid element as a function of an accumulated temperature index, while Cazorzi and Fontana (1996) and Hock (1999) incorporate clear-sky shortwave radiation to account for the spatial heteorogeneity of radiation and melt conditions in complex terrain.

IV Discussion and concluding remarks

Due to the availability of air temperature data, temperature-index methods will probably remain the most widely used approach to compute melt for many purposes. These methods lump the surface energy exchange into one or a few parameters, with the disadvantage that melt factors vary from site to site, so model calibration is required. Conversely, energy-balance melt models more properly describe the physical processes at the glacier surface but require much more data, which are often not available.

There is a trend to replace simpler schemes with more sophisticated ones. However, a fundamental question concerns whether such an increase in sophistication is warranted. In Figure 2, hourly discharge simulations for Storglaciären, Sweden, based on different melt models are intercompared. Clearly, the classical degree-day model captures the seasonal pattern in discharge but not the daily discharge fluctuations (Figure 2a). Model performance is significantly enhanced by incorporating potential direct solar radiation as an index of local and daily variability in the energy available for melt (Figure 2b). Although this model assumes clear-sky conditions, a third approach including measured global radiation to incorporate cloud effects does not yield any improvement in performance (Figure 2c; Hock, 1999). This is probably due to increases in other energy fluxes under cloudy conditions, such as long-wave irradiance. Both energy-balance approaches (Figure 2d and e) yield good results. The models differ in their levels of sophistication. Model (d) assumes a melting

surface, constant snow albedo and spatially invariant longwave irradiance, while model (e) parameterizes these quantities, thus accounting for spatial variability (Hock, 1998). In general, model performance improved with increasing model complexity.

For runoff modelling using spatially lumped models and typical time steps of one day, modelling intercomparison projects (e.g., WMO, 1986) revealed that model complexity could not be related to the quality of the simulation results. Simple models provided comparable results to more sophisticated models, which is generally attributed to the difficulties of assigning proper model parameters and meteorological input data to each catchment element. The example in Figure 2 indicates that the appropriate level of model sophistication is related to the temporal and spatial scale of interest and the objectives of the study. For catchment-scale studies employing daily time steps, simple temperature-index methods are often sufficient. However, if higher resolution in space and time is required, more sophisticated energy-balance models are preferable. Physically based models are more suited to quantifying the response of melt and discharge to future climate changes since parameters in simpler models may not be the same under a different climate. In highly glacierized basins, a higher (e.g., hourly) temporal resolution is necessary for accurate runoff modelling especially with respect to peak flow estimates, because of the enormous melt-induced diurnal discharge fluctuations. This aspect of temporal resolution is crucial in attempts to predict the changes associated with a warming climate, as diurnal melt-cycles are expected to be amplified, significantly increasing peak flows (Hock *et al.*, 2005). The spatial aspect is important in complex topography in mass balance studies as well as in studies related to avalanche forecasting, erosion, solifluction, solute transport or vegetation patterns.

Generally speaking, significant advances in distributed melt modelling have been made in recent years, based on both temperature-index
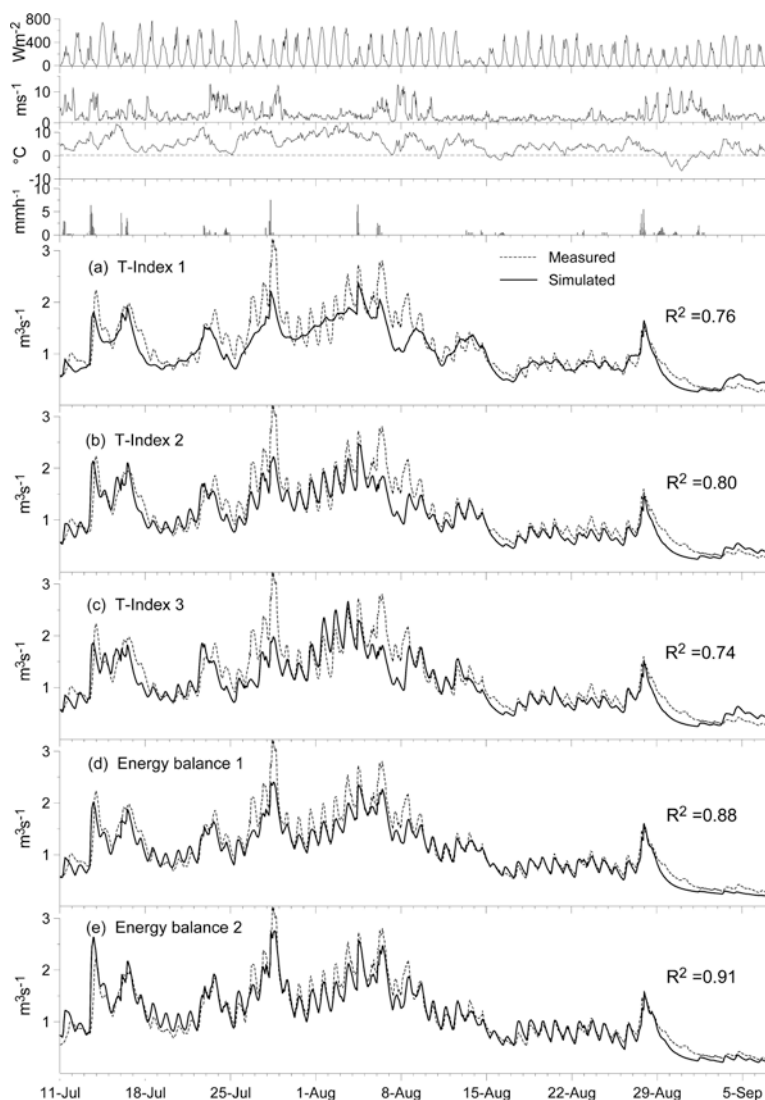
Figure 2   Simulated and measured hourly discharge (m³ s⁻¹) of Storglaciären, Sweden, using different temperature-index and energy-balance models for the melt modelling and a linear reservoir model for water routing. Melt calculations are based on the classical degree-day method (a), a modified temperature-index model including potential direct solar radiation (b), a modified temperature-index model including potential direct solar radiation and global radiation (c), a simple energy-balance model (d) and a more sophisticated energy-balance model (e). Model performance is given in terms of the efficiency criterion R^2 (Nash and Sutcliffe, 1970). Also given are hourly measurements of global radiation (Wm²), wind speed (m s⁻¹), air temperature (°C) and precipitation (mm h⁻¹)
Source: Models (a–c) from Hock (1999); model (d) from Hock and Noetzli (1997); model (e) from Hock (1998).

and energy-balance methods. Such app-
roaches require further testing and refine-
ment and would benefit from more extensive
exploitation of increasingly available of
remote sensing data, for both model input
and verification. The need to extrapolate
meteorological input data places major limita-
tions on the quality of model simulations
(Charbonneau *et al.*, 1981). Often, wind
speed and relative humidity are assumed spa-
tially constant and air temperature is varied
with altitude according to a simple lapse rate.
The inclusion of wind models may aid in
better interpolating meteorological input
data, although the interfacing may be difficult
due to differences in spatial resolution.

Energy-balance models yield sufficiently
accurate estimates of the spatial and toporal
patterns of incoming radiation in mountain
terrain. However, the determination of tur-
bulent fluxes and surface albedo are currently
identified as the most prominent uncertain-
ties. Increasing evidence suggests that exist-
ing boundary layer theory does not apply over
the typically inclined glacier surface, which is
subject to gravity winds. Much uncertainty
concerns the determination of exchange
coefficients and the consideration of stability
effects. Evidence seems to mount that the
turbulent heat fluxes over valley glaciers
are larger than existing theory predicts.
Further research needs to be directed
towards the development of realistic con-
cepts in the glacier environment based on
careful re-evaluation of existing data sets
and, in particular, more eddy correlation
studies on valley glaciers. Determining accu-
rate spatial distributions of turbulent fluxes
is an even larger challenge that needs to
be tackled. Besides the problems in data
extrapolation, accounting for the spatial
and temporal variations in exchange coeffi-
cients is a yet rather unexplored issue.
Despite a large variety of proposed albedo
parameterizations, future research needs to
focus on quantifying physical controls on
glacier albedo and the development of
models capturing the full range of spatial and
temporal albedo variability. In addition,
energy gain due to advected heat may not be
negligible on valley glaciers and needs further
investigation.

Few studies have attempted to link the
variations in ablation and energy partitioning
at the point scale to larger-scale atmospheric
conditions (e.g., Hoinkes, 1968; Cline, 1997;
Hannah *et al.*, 1999). Such relationships may
be exploited for forecasting the timing of melt-
induced runoff from mountainous regions, as
large-scale air mass characteristics are more
predictable than local wind, temperature and
relative humidity patterns. Further research
will need to focus on the links between the
different energy fluxes and the synoptic
weather pattern, and investigate their poten-
tial for operational use in melt forecasting.

References

Ahlmann, H.W. 1935: Scientific results of the
   Norwegian-Swedish Spitzbergen expedition 1934,
   Part 5: The Fourteenth of July Glacier. *Geografiska
   Annaler* 17, 167–218.
— 1948: *Glaciological Research on the north Atlantic
   coasts*. Research Series No. 1. London: Geographical
   Society, 83 pp.
Ambach, W. 1963: Untersuchungen zum Energieumsatz
   in der Ablationszone des grönländischen Inlandeises.
   Meddelser om Grønland 174(4), 311 pp.
— 1986: Nomographs for the determination of meltwater
   from snow and ice surfaces. *Berichte des naturwis-
   senschaftlich-medizinischen Vereins in Innsbruck* 73, 7–15.
— 1988: Interpretation of the positive-degree-days
   factor by heat balance characteristics – West
   Greenland. *Nordic Hydrology* 19, 217–24.
Ambach, W. and **Hoinkes, H.C.** 1963: *The heat
   balance of an Alpine snowfield (Kesselwandferner
   3240 m, Oetztal Alps, 1958)*. Wallingford: IAHS
   Publication 61, 24–36.
Anderson, E.A., 1972: Techniques for predicting snow
   cover runoff. In *The role of snow and ice in hydrology,*
   Proceedings of the Banff Symposium 1972,
   Wallingford: IAHS Publication 107, 840–63.

— 1973: *National weather service river forecast system/ snow accumulation and ablation model*. NOAA Technical Memorandum NWS HYDRO-17. Silver Spring, MD: US Department of Commerce, 217 pp.

— 1976: *A point energy and mass balance model of a snow cover*. NOAA Technical Report NWS 19. Washington, DC: NOAA, 150 pp.

Andreas, E.L. 1987: A theory for the scalar roughness and the scalar transfer coefficient over snow and sea ice. *Boundary-Layer Meteorology* 38, 159–84.

Ångström, A. 1916: Über die Gegenstrahlung der Atmosphäre. *Meteoroische Zeitschrift* 33, 529–38.

— 1933: On the dependence of ablation on air temperature, radiation and wind. *Geografiska Annaler* 15, 264–71.

Arendt, A. and **Sharp, M.** 1999: Energy balance measurements on a Canadian high arctic glacier and their implications for mass balance modelling. In Tranter, M., Armstrong, R., Brun, E., Jones, G., Sharp, M. and Williams, M., editors, *Interactions between the cryosphere, climate and greenhouse gases,* Proceedings of the IUGG Symposium, Birmingham 1999, Wallingford: IAHS Publication 256, 165–72.

Arnold, N.S., Willis, I.C., Sharp, M.J., Richards, K.S. and **Lawson, W.J.** 1996: A distributed surface energy-balance model for a small valley glacier. I. Development and testing for Haut Glacier d'Arolla, Valais, Switzerland. *Journal of Glaciology* 42, 77–89.

Bader, H. and **Weilenmann, P.** 1992: Modeling temperature distribution, energy and mass flow in a (phase-changing) snowpack. I. Model and case studies. *Cold Regions Science and Technology* 20, 157–81.

Beljaars, A.C.M. and **Holtslag, A.A.M.** 1991: Flux parameterization over land surfaces for atmospheric models. *Journal of Applied Meteorology* 30, 327–41.

Bergström, S. 1976: Development and application of a conceptual runoff model for Scandinavian catchments. Department of Water Resources Engineering, Lund Institute of Technology/University of Lund, Bulletin Series A 52, 134 pp.

Bintanja, R. 1999: On the glaciological, meteorological, and climatological significance of Antarctic blue ice areas. *Reviews of Geophysics* 37, 337–59.

Bintanja, R. and **van den Broeke, M.R.** 1995: Momentum and scalar transfer coefficients over aerodynamically smooth Antarctic surfaces. *Boundary-Layer Meteorology* 74, 89–111.

Blöschl, G., Kirnbauer, B. and **Gutknecht, D.** 1991: Distributed snowmelt simuations in an Alpine catchment. I. Model evaluation on the basis of snow cover patterns. *Water Resources Research* 27, 3171–79.

Bøggild, C.E., Knudby, C.J., Knudsen, M.B. and **Starzer, W.** 1999: Snowmelt and runoff modelling of an arctic hydrological basin in east Greenland. *Hydrological Processes* 13, 1989–2002.

Braithwaite, R.J. 1995a: Aerodynamic stability and turbulent sensible-heat flux over a melting ice surface, the Greenland ice sheet. *Journal of Glaciology* 41, 562–71.

— 1995b: Positive degree-day factors for ablation on the Greenland ice sheet studied by energy-balance modelling. *Journal of Glaciology* 41, 153–60.

Braithwaite, R.J. and **Olesen, O.B.** 1990a: Response of the energy balance on the margin of the Greenland ice sheet to temperature changes. *Journal of Glaciology* 36, 217–21.

— 1990b: A simple energy-balance model to calculate ice ablation at the margin of the Greenland ice sheet. *Journal of Glaciology* 36, 222–28.

Braithwaite, R.J. and **Thomsen, O.O.** 1989: Simulation of run-off from the Greenland ice sheet for planning hydro-electric power, Ilulissat/ Jakobshavn, West Greenland. *Annals of Glaciology* 13, 12–15.

Braithwaite, R.J. and **Zhang, Y.** 1999: Modelling changes in glacier mass balance that may occur as a result of climate changes. *Geografiska Annaler* 81A, 489–496.

Braithwaite, R.J., Konzelmann, T., Marty, C. and **Olesen, O.B.** 1998: Reconnaisance study of glacier energy balance in north Greenland, 1993–94. *Journal of Glaciology* 44, 239–247.

Braun, L.N. and **Aellen, M.** 1990: Modelling discharge of glacierized basins assisted by direct measurements of glacier mass balance. In Lang, H. and Musy, A. editors, *Hydrology of mountainous regions I,* Proceedings of two Lausanne Symposia, 1990, Wallingford: IAHS Publication 193, 99–106.

Braun, L.N., Aellen, M., Funk, M., Hock, R., Rohrer, M.B., Steinegger, U., Kappenberger, G., and **Müller-Lemans, H.** 1994: Measurement and simulation of high alpine water balance components in the Linth-Limmern head watershed (Northeastern Switzerland). *Zeitschrift für Gletscherkunde und Glazialgeologie* 30, 161–85.

Braun, L.N., Grabs, W. and **Rana, B.** 1993: Application of a conceptual precipitation-runoff model in the Langtang Khola basin, Nepal Himalaya. In Young, G.J., editor, *Snow and glacier hydrology,* Proceedings of the Kathmandu Symposium 1992, Wallingford: IAHS Publication 218, 221–37.

Brock, B., Willis, I.C. and **Sharp, M.J.** 2000a: Measurement and parameterization of albedo variations at Haut Glacier d'Arolla, Switzerland. *Journal of Glaciology* 155, 675–88.

Brock, B., Willis, I.C., Sharp, M.J. and **Arnold, N.S.** 2000b: Modelling seasonal and spatial variations in the surface energy balance of Haut Glacier d'Arolla, Switzerland. *Annals of Glaciology* 31, 53–62.

Brubaker, K., Rango, A. and **Kustas, W.** 1996: Incorporating radiation inputs into the snowmelt runoff model. *Hydrological Processes* 10, 1329–43.

Brun, E., Martin, E., Simon, V., Gendre, C. and **Coleou, C.** 1989: An energy and mass model of snow cover suitable for operational avalanche forecasting. *Journal of Glaciology* 35, 333–42.

Brunt, D. 1932: Notes on radiation in the atmosphere I. *Quartely Journal of the Royal Meteorological Society* 58, 389–420.

Brutsaert, W. 1975: On a derivable formula for long-wave radiation from clear skies. *Water Resources Research* 11, 742–44.

Burlando, P., Pellicciotti, F. and **Strasser, U.** 2002: Modelling mountainous water systems. Between learning and speculating. Looking for challenges. *Nordic Hydrology* 33, 47–74.

Calanca, P. 2001: A note on the roughness length for temperature over melting snow and ice. *Quarterly Journal of the Royal Meteorological Society* 127, 255–60.

Cazorzi, F. and **Fontana, G.D.** 1996: Snowmelt modelling by combining air temperature and a distributed radiation index. *Journal of Hydrology* 181, 169–87.

Charbonneau, R., Lardeau, J.P. and **Obled, C.** 1981: Problems of modelling a high mountainous drainage basin with predominant snow yields. *Hydrological Sciences Bulletin* 26, 345–61.

Choudhury, B.J. and **Chang, A.T.C.** 1981: On the angular variation of solar reflectance of snow. *Journal of Geophysical Research* 86, 465–72.

Cline, D.W. 1997: Snow surface energy exchanges and snowmelt at a continental, midlatitude Alpine site. *Water Resources Research* 33, 689–701.

Colbeck, S.C. 1972: A theory of water percolation in snow. *Journal of Glaciology* 11, 369–85.

Collares-Pereira, M. and **Rabl, A.** 1979: The average distribution of solar radiation correlations between diffuse and hemispherical and between daily and hourly insolation values. *Solar Energy* 22, 155–164.

Corps of Engineers 1956: *Summary report of the snow investigations, snow hydrology*. Portland, OR: US Army Engineer Division, 437pp.

Crawford, N. 1973: Computer simulation techniques for forecasting snowmelt runoff. In *The role of snow and ice in hydrology,* Proceedings of the Banff Symposium 1972, Wallingford: IAHS Publication 107, 1062–72.

Cutler, P. and **Munro, D.S.** 1996: Visible and near-infrared reflectivity during the ablation period on Peyto Glacier, Alberta, Canada. *Journal of Glaciology* 42, 333–40.

Daly, S.F., Davis, R., Ochs, E. and **Pangburn, T.** 2000: An approach to spatially distributed snow modelling of the Sacramento and San Joaquin basins, California. *Hydrological Processes* 14, 3257–71.

de la Casinier, A.C. 1974: Heat exchange over a melting snow surface. *Journal of Glaciology* 13, 55–72.

de Quervain, M. 1951: Zur Verdunstung der Schneedecke. *Archiv für Meteorologie, Geophysik und Bioklimatologie* B3, 47–64.

Denby, B. and **Greuell, W.** 2000: The use of bulk and profile methods for determining surface heat fluxes in the presence of glacier winds. *Journal of Glaciology* 46, 445–452.

Dozier, J. 1980: A clear-sky spectral solar radiation model for snow-covered mountainous terrain. *Water Resources Research* 16, 709–18.

— 1987: Recent research in snow hydrology. *Reviews of Geophysics* 25, 153–161.

Dunn, S.M. and **Colohan, R.J.E.** 1999: Developing the snow component of a distributed hydrological model: a step-wise approach based on multi-objective analysis. *Journal of Hydrology* 223, 1–16.

Dyer, A.J. 1974: A review of flux-profile relationships. *Boundary-Layer Meteorology* 7, 363–72.

Ellingson, R.G., Ellis, J. and **Fels, S.** 1991: The inter-comparison of radiation codes used in climate models: long-wave results. *Journal of Geophysical Research* 96, 8929–53.

Escher-Vetter, H. 1985a: Energy balance calculations for the ablation period 1982 at Vernagtferner, Oetztal Alps. *Annals of Glaciology* 6, 158–60.

— 1985b: Energy balance calculations from five years meteorological records at Vernagtferner, Oetztal Alps. *Zeitschrift für Gletscherkunde und Glazialgeologie* 21, 397–402.

— 2000: Modelling meltwater producton with a distributed energy balance method and runoff using a linear reservoir approach – results from Vernagtferner, Oetztal Alps, for the ablation seasons 1992 to 1995. *Zeitschrift für Gletscherkunde und Glazialgeologie* 36, 119–50.

Essery, R. 1999: Parameterization of heterogeneous snowmelt. *Theoretical Applied Climatology* 62, 25–30.

Finsterwalder, S. 1897: Der Vernagtferner. *Wissenschaftliche Ergänzungshefte zur Zeitschrift des Deutschen und Oesterreichischen Alpenvereins* 1(1), 1–112.

Finsterwalder, S. and **Schunk, H.** 1887: Der Suldenferner. *Zeitschrift des Deutschen und Oesterreichischen Alpenvereins* 18, 72–89.

Föhn, P.M.B. 1973: Short-term snow melt and ablation derived from heat- and mass-balance measurements. *Journal of Glaciology* 12, 275–289.

Forrer, J. and **Rotach, M.** 1997: On the turbulence structure in the stable boundary layer over the Greenland ice sheet. *Boundary-Layer Meteorology* 85, 111–36.

Funk, M. 1985: Räumliche Verteilung der Massenbilanz auf dem Rhonegletscher und ihre Beziehung zu Klimaelementen. *Zürcher Geographische Schriften* 24, Department of Geography, ETH Zürich, 183 pp.

Garnier, B. and **Ohmura, A.** 1968: A method of calculating the direct shortwave radiation income on slopes. *Journal of Applied Meteorology* 7, 796–800.

Grainger, M.E. and **Lister, H.** 1966: Wind speed, stability and eddy viscosity over melting ice surfaces. *Journal of Glaciology* 6, 101–27.

Greuell, W. and **Konzelmann, T.** 1994: Numerical modelling of the energy balance and the englacial temperature of the Greenald ice sheet. Calculations for the ETH-camp location (West Greenland, 1155 m a.s.l.). *Global Planetary Change* 9, 91–114.

Greuell, W. and **Oerlemans, J.** 1987: Sensitivity studies with a mass balance model including temperature profile calculations inside the glacier. *Zeitschrift für Gletscherkunde und Glazialgeologie* 22, 101–24.

— 1989: Energy balance calculations on and near Hintereisferner (Austria) and an estimate of the effect of greenhouse warming on ablation. In Oerlemans, J., editor, *Glacier fluctuations and climatic change*, Glaciology and Quaternary Geology, Dordrecht:Kluwer, 305–23.

Greuell, W., Knap, W.H. and **Smeets, P.C.** 1997: Elevational changes in meteorological variables along a mid-latitude glacier during summer. *Journal of Geophysical Research* 102(D22), 25941–54.

Halberstam, I. and **Schieldge, J.P.** 1981: Anomalous behaviour of the atmospheric surface layer over a melting snow pack. *Journal of Applied Meteorology* 20, 255–65.

Hannah, M., Gurnell, A.M. and **McGregor, G.R.** 1999: Indentifying links between large-scale atmospheric circulation and local glacier ablation climates in the French Pyrenees. In Tranter, M., Armstrong, R., Brun, E., Jones, G., Sharp, M. and Williams, M., editors, *Interactions between the cryosphere, climate and greenhouse gases*, Proceedings of the IUGG Symposium, Birmingham 1999, Wallingford: IAHS Publication 256, 155–63.

Harding, R.J., Entrasser, N., Escher-Vetter, H., Jenkins, A., Kaser, M., Kuhn, M., Morris, E.M. and **Tanzer, G.** 1989: Energy and mass balance studies in the firn area of the Hintereisferner. In Oerlemans, J. editor, *Glacier fluctuations and climatic change*, Glaciology and Quaternary Geology, Dordrecht: Kluwer, 325–41.

Hay, J.E. and **Fitzharris, B.B.** 1988: A comparison of the energy-balance and bulk-aerodynamic approaches for estimating glacier melt. *Journal of Glaciology* 34, 145–53.

Herzfeld, U., Mayer, H., Feller, W. and **Mimler, M.** 2000: Geostatistical analysis of glacier-roughness data. *Annals of Glaciology* 30, 235–42.

Hess, H. 1904: *Die Gletscher*. Braunschweig: Druck und Verlag von Friedrich Vieweg und Sohn, 426 pp.

Hock, R. 1998: Modelling of glacier melt and discharge. *Zürcher Geographische Schriften* 70, Department of Geography, ETH Zürich, 140pp.

— 1999: A distributed temperature-index ice- and snowmelt model including potential direct solar radiation. *Journal of Glaciology* 45, 101–11.

— 2003: Temperature index melt modelling in mountain areas. *Journal of Hydrology* 282(1-4), 104–15 Doi: 10.1016/S0022-1694(03)00257-9.

Hock, R. and **Holmgren, B.** 1996: Some aspects of energy balance and ablation of Storglaciären, Sweden. *Geografiska Annaler* 78A, 121–31.

— 2005: A distributed energy balance model for complex topography and its application to Storglaciären, Sweden. *Journal of Glaciology,* in press.

Hock, R. and **Noetzli, C.** 1997: Areal melt and discharge modelling of Storglaciären, Sweden. *Annals of Glaciology* 24, 211–17.

Hock, R., Jansson, P. and **Braun, L.** 2005: Modelling the response of mountain glacier discharge to climate warming. In Huber, U.M., Reasoner, M.A. and Bugmann, H. editors, *Global change and mountain regions – a state of knowledge overview*, Advances in Global Change Series, Dordrecht: Springer, 293–52.

Hoeck, E. 1952: Der Einfluss der Strahlung und der Temperatur auf den Schmelzprozess der Schneedecke. *Beiträge zur Geologie der Schweiz – Geotechnische Serie – Hydrologie*, Bern, 36 pp.

Hogg, I.G.G., Paren, J.G. and **Timmis, R.J.** 1982: Summer heat and ice balances on Hodges glacier, south Georgia, Falkland dependencies. *Journal of Glaciology* 28, 221–38.

Högström, U. 1988: Non-dimensional wind and temperature profiles in the atmospheric surface layer: a re-evaluation. *Boundary-Layer Meteorology* 42, 55–78.

Hoinkes, H.C. 1955: Measurements of ablation and heat balance on alpine glaciers. *Journal of Glaciology* 2, 497–501.

— 1968: Glacier variation and weather. *Journal of Glaciology* 7, 3–19.

— 1969: Surges of the Vernagtferner in the Oetztal Alps since 1599. *Canadian Journal of Earth Science* 6, 853–61.

Hoinkes, H.C. and **Steinacker, H.** 1975: Hydrometeorological implications of the mass balance of Hintereisferner, 1952–53 to 1968–69. In *Proceedings of the Snow and Ice Symposium, Moscow 1971,* Wallingford: IAHS Publication 104, 144–49.

Hoinkes, H.C. and **Untersteiner, N.** 1952: Wärmeumsatz und Ablation auf Alpengletschern I. Vernagtferner (Oetztaler Alpen), August 1950. *Geografiska Annaler* 34(1-2), 99–158.

Holmgren, B. 1971: *Climate and energy exchange on a sub-polar ice cap in summer. Arctic Institute of North America Devon Island Expedition 1961-1963*. Uppsala: Meteorologiska Institutionen, Uppsala Universitet. Meddelande 107 Part A–E.

Inoue, J. 1989: Surface drag over the snow surface of the Antarctic plateau 1: factors controlling surface drag over the katabatic wind region. *Journal of Geophysical Research* 94(D2), 2207–2217.

Iqbal, M. 1983: *An introduction to solar radiation*. London: Academic Press, 390 pp.

Jackson, B.S. and **Carroll, J.J.** 1978: Aerodynamic roughness as a function of wind direction over asymmetric surface elements. *Boundary-Layer Meteorology* 14, 323–30.

Jansson, P., Hock, R. and **Schneider, T.** 2003: The concept of glacier storage – a review. *Journal of Hydrology* 282, 115–29, 10.1016/S0022-1694(03)00258-0.

Jonsell, U., Hock, R. and **Holmgren, B.** 2003: Spatial and temporal variations in albedo on stoglaciären. *Journal of Glaciology* 49, 59–68.

Jordan, R. 1991: A one-dimensional temperature model for a snow cover: technical documentation for SNTHERM 89. *CRREL Special Report*, 91–16.

Kane, D.L. and **Gieck, R.E.** 1997: Snowmelt modeling at small Alaskan arctic watershed. *Journal of Hydrological Engineering*, 2, 204–10.

Kasten, F. 1983: Parameterisierung der Globalstrahlung durch Bedeckungsgrad und Trübungsfaktor. *Annalen der Meteorologie* 20, 49–50.

Kattelmann, R. and **Yang-Daqing, Y.** 1992: Factors delaying spring runoff in the upper Urumqi River basin, China. *Annals of Glaciology* 16, 225–30.

King, J.C. and **Anderson, P.S.** 1994: Heat and water vapour fluxes and scalar roughness lengths over an Antarctic ice shelf. *Boundary-Layer Meteorology* 69, 101–21.

Kirnbauer, R., Blöschl, G. and **Gutknecht, D.** 1994: Entering the era of distributed snow models. *Nordic Hydrology* 25, 1–24.

Klok, E.J. and **Oerlemans, J.** 2002: Model study of the spatial distribution of the energy and mass balance of Morteratschgletscher, Switzerland. *Journal of Glaciology* 48, 505–18.

Koenig-Langlo, G. and **Augstein, F.** 1994: Parameterization of the downward long-wave radiation at the Earth's surface in polar regions. *Meteorologische Zeitschrift* 3, 343–47.

Kondratyev, K.Y. 1965: *Radiative heat exchange in the atmosphere*. Oxford: Pergamon Press, 411 pp.

— 1969: *Radiation in the atmosphere*. New York: Academic Press, 912 pp.

König, M., Wadham, J., Winther, J.G., Kohler, J. and **Nuttall, A.M.** 2002: Detection of superimposed ice on the glaciers Kongsvegen and midre Lovenbreen, Svalbard, using SAR satellite imagery. *Annals of Glaciology* 34, 335–42.

Konya, K., Matsumoto, T. and **Naruse, R.** 2004: Surface heat balance and spatially distributed ablation modelling at Koryto Glacier, Kamchatka peninsula, Russia. *Geografiska Annaler* 86A, 337–48.

Konzelmann, T. and **Braithwaite, R.J.** 1995: Variations of ablation, albedo and energy balance at the margin of the Greenland ice sheet, Kronprins Christian Land, eastern north Greenland. *Journal of Glaciology* 41, 174–82.

Konzelmann, T. and **Ohmura, A.** 1995: Radiative fluxes and their impact on the energy balance of the Greenland ice sheet. *Journal of Glaciology* 41, 490–502.

Konzelmann, T., van de Wal, R.S.W., Greuell, W., Bintanja, R., Henneken, E.A.C. and **Abe-Ouchi, A.** 1994: Parameterization of global and longwave incoming radiation for the Greenland ice sheet. *Global Planetary Change* 9, 143–64.

Kuhn, M. 1984: Physikalische Grundlagen des Energie- und Massenhaushalts der Schneedecke. In Brechtel, H., editor, *Schneehydrologische Forschung in Mitteleuropa*, volume 7, DVWK (Deutscher Verband für Wasserwirtschaft und Kulturbau), 5–56.

— 1987: Micro-meteorological conditions for snow melt. *Journal of Glaciology* 33, 263–72.

— 1993: Methods of assessing the effects of climatic changes on snow and glacier hydrology. In Young, G.J., editor, *Snow and glacier hydrology,* Proceedings of the Kathmandu Symposium 1992, Wallingford: IAHS Publication 218, 135-44.

Kustas, W.P. and **Rango, A.** 1994: A simple energy budget algorithm for the snowmelt runoff model. *Water Resources Research* 30, 1515–27.

Kuusisto, E. 1980: On the values and variability of degree-day melting factors in Finland. *Nordic Hydrology* 11, 235–42.

Kuzmin, P.P. 1961: Melting of snow cover. *Israel Program for Scientific Translation*, 290 pp.

La Chapelle, E. 1959: Annual mass and energy exchange on the Blue Glacier. *Journal of Geophysical Research* 64, 443–49.

— 1961: Energy exchange measurements on the Blue Glacier, Washington. *IAHS Publication* 54, 302–10.

Lang, H. 1981: Is evaporation an important component in high alpine hydrology? *Nordic Hydrology* 12, 217–24.

— 1986: Forecasting meltwater runoff from snow-covered areas and from glacier basins. In Kraijenhoff, D.A. and Moll, J.R., editor, *River flow modelling and forecasting*, Dordrecht: D. Reidel, 99–127.

Laumann, T. and **Reeh, N.** 1993: Sensitivity to climate change of the mass balance of glaciers in southern Norway. *Journal of Glaciology* 39, 656–65.

Lettau, H. 1939: *Atmosphä̈rische Turbulenz*. Leipzig: Akademische Verlagsgesellschaft.

— 1969: Note on aerodynamic roughness-parameter estimation on the basis of roughness-element description. *Journal of Applied Meteorology* 8, 828–32.

List, R.J. 1966: *Smithsonian Meteorological Tables* (sixth revised edition). Washington, DC: Smithsonian. Institution.

Lütschg-Loetscher, O. 1944: Zum Wasserhaushalt des Schweizer Hochgebirges. *Beiträge zur Geologie der Schweiz – Geotechnische Serie – Hydrologie* 1(1), Bern, 101 pp.

Male, D.H. 1980: The seasonal snow cover. In Colbeck, S., editor, *Dynamics of snow and ice masses*, New York: Academic Press, 305–91.

Male, D.H. and **Granger, R.J.** 1981: Snow surface and energy exchange. *Water Resources Research* 17, 609–27.

Marcus, M.G., Moore, R.D. and **Owens, I.F.** 1984: Short-term estimates of surface energy transfers and ablation on the lower Franz Josef Glacier, South Westland New Zealand. *New Zealand Journal of Geology and Geophysics* 28, 559–67.

Marks, D. and **Dozier, J.** 1979: A clear-sky longwave radiation model for remote alpine areas. *Archiv für Meterologie, Geophysik und Bioklimatologie* 27, 159–78.

— 1992: Climate and energy exchange at the snow surface in the alpine region of the Sierra Nevada. 2. Snow cover energy balance. *Water Resources Research* 28, 3042–54.

Marsh, P. and **Pomeroy, J.W.** 1997: Sensible heat flux and local advection over a heterogeneous landscape at an Arctic tundra site during snowmelt. *Annals of Glaciology* 25, 132–36.

Marshall, S.E. and **Warren, S.G.** 1987: Parameterization of snow albedo for climate models. In Goodison, B.E., Barry, R.G. and Dozier, J., editors, *Large scale effects of seasonal snow cover,* Proceedings of the Vancouver Symposium 1987, Wallingford: IAHS Publication 166, 43–50.

Martin, E. and **Lejeune, Y.** 1998: Turbulent fluxes above the snow surface. *Annals of Glaciology* 26, 179–83.

Martin, S. 1975: Wind regimes and heat exchange on glacier de Saint-Sorlin. *Journal of Glaciology* 14, 91–105.

Martinec, J. 1989: Hour-to-hour snowmelt rates and lysimeter outflow during an entire ablation period. In Colbeck, S.C., editor, *Glacier and snow cover variations,* Proceedings of the Baltimore Symposium, Maryland 1989, Wallingford: IAHS Publication 183, 19–28.

Martinec, J. and **Rango, A.** 1986: Parameter values for snowmelt runoff modelling. *Journal of Hydrology* 84, 197–219.

Moore, R. 1983: On the use of bulk aerodynamic formulae over melting snow. *Nordic Hydrology* 14, 193–206.

Moore, R.D. 1991: A numerical simulation of supraglacial heat advection and its influence on ice melt. *Journal of Glaciology* 37, 296–300.

Morris, E.M. 1989: Turbulent transfer over snow and ice. *Journal of Hydrology* 105, 205–23.

Morris, E.M., Anderson, P.S., Bader, H., Weilenmann, P. and **Blight, C.** 1994: Modelling mass and energy exchange over polar snow using the DAISY model. In Jones, H.G., Davies, T.D., Ohmura, A. and Morris, E.M., editors, *Snow and ice covers: interactions with the atmosphere and ecosystems,* Proceedings of the Yokohama Symposium 1993, Wallingford: IAHS Publication 223, 53–60.

Müller, F. and **Keeler, C.M.** 1969: Errors in short-term ablation measurements on melting ice. *Journal of Glaciology* 8, 91–105.

Müller, H. 1985: Review paper: on the radiation budget in the Alps. *Journal of Climatology* 5, 445–62.

Munro, D.S. 1989: Surface roughness and bulk heat transfer on a glacier: comparison with eddy correlation. *Journal of Glaciology* 35, 343–48.

— 1990: Comparison of melt energy computations and ablatometer measurements on melting ice and snow. *Arctic and Alpine Research* 22, 153–62.

Munro, D.S. and **Davies, J.A.** 1972: An experimental study of the glacier boundary layer over melting ice. *Journal of Glaciology* 18, 425–36.

Munro, D.S. and **Young, G.J.** 1982: An operational net shortwave radiation model for glacier basins. *Water Resources Research* 18, 220–30.

Nash, J.E. and **Sutcliffe, J.V.** 1970: River flow forecasting through conceptual models. Part I – a discussion of principles. *Journal of Hydrology* 10, 282–90.

Obukhov, A.M. 1946: Turbulentnost' v temeraturno-neodnorodnoy atmosfere (Turbulence in the thermally inhomogeneous atmosphere). *Trudy Instituta Teoreticheskoyi Geofiziki, Akademiya Nauk SSSR* 1, 95–115.

Oerlemans, J. 1992: Climate sensitivity of glaciers in southern Norway: application of an energy-balance model to Nigardsbreen, Hellstugubreen and Alfotbreen. *Journal of Glaciology* 38, 223–32.

— 2000: Analysis of a 3-year meteorological record from the ablation zone of Moteratschgletscher, Switzerland: energy and mass balance. *Journal of Glaciology* 46, 571–79.

Oerlemans, J. and **Fortuin, J.P.** 1992: Sensitivity of glaciers and small ice caps to greenhouse warming. *Science* 258, 115–17.

Oerlemans, J. and **Grisogono, B.** 2002: Glacier winds and parameterisation of the related surface heat fluxes. *Tellus* 54A, 440–52.

Oerlemans, J., Anderson, B., Hubbard, A., Huybrechts, P., Johannesson, T., Knap, W.H. and **Schmeits, M.** 1998: Modelling the response of glaciers to climate warming. *Climate Dynamics* 14, 267–74.

Ohata, T. 1989: The effect of glacier wind on local climate, turbulent heat fluxes and ablation. *Zeitschrift für Gletscherkunde und Glazialgeologie* 25, 49–68.

Ohmura, A. 1981: Climate and energy balance on arctic tundra. Axel Heiberg Island, Canadian Arctic Archipelago, spring and summer 1969, 1970 and 1972. *Zürcher Geographische Schriften* 3, Department of Geography, ETH Zürich, 448 pp.

— 2001: Physical basis for the temperature-based melt-index method. *Journal of Applied Meteorology* 40, 753–61.

Ohmura, A., Kasser, P. and **Funk, M.** 1992: Climate at the equilibrium line of glaciers. *Journal of Glaciology* 38, 397–411.

Ohmura, A., Konzelmann, T., Rotach, M., Forrer, J., Wild, M., Abe-Ouchi, A. and **Toritani, H.** 1994: Energy balance for the Greenland ice sheet by observation and model computation. In Jones, H.G., Davies, T.D., Ohmura, A. and Morris, E.M., editors, *Snow and ice covers: interactions with the atmosphere and ecosystems,* Proceedings of the Yokohama Symposium 1993, Wallingford: IAHS Publication 223, 163-74.

Ohta, T. 1994: A distributed snowmelt prediction model in mountain areas based on an energy balance method. *Annals of Glaciology* 19, 107–13.

Oke, T.R. 1987: *Boundary layer climates* (second edition). London: Routledge, 435 pp.

Olyphant, G. 1986: Longwave radiation in mountainous areas and its influence on the energy balance of alpine snowfields. *Water Resources Research* 22, 62–66.

Olyphant, G.A. and **Isard, S.A.** 1988: The role of advection in the energy balance of late-lying snowfields: Niwot Ridge, Front Range, Colorado. *Water Resources Research* 24, 1962–68.

Orvig, S. 1954: Glacio-meteorological observations on icecaps in Baffin Island. *Geografiska Annaler* 36, 197–318.

Paterson, W.S.B. 1994: *The physics of glaciers* (third edition). Oxford: Pergamon Press, 480 pp.

Plüss, C. 1997: The energy balance over an alpine snowcover. *Zürcher Geographische Schriften* 65, Department of Geography, ETH Zürich, 115 pp.

Plüss, C. and **Mazzoni, R.** 1994: The role of turbulent heat fluxes in the energy balance of high alpine snow cover. *Nordic Hydrology* 25, 25–38.

Plüss, C. and **Ohmura, A.** 1997: Longwave radiation on snow-covered mountainous surfaces. *Journal of Applied Meteorology* 36, 818–24.

Prandtl, L. 1934: *The mechanics of viscous fluids* (*Aerodynamic theory*) Berlin: Durand (ed.), vol. III, division G.

Price, A.G. and **Dunne, T.** 1976: Energy balance computations of snowmelt in a subarctic area. *Water Resources Research* 12, 686–94.

Quick, M.C. and **Pipes, A.** 1977: UBC watershed model. *Hydrological Sciences Bulletin* 221, 153–61.

Rango, A. and **Martinec, J.** 1995: Revisiting the degree-day method for snowmelt computations. *Water Resources Bulletin* 31, 657–69.

Reeh, N., Mohr, J.J., Krabill, W.B., Thomas, R., Oerter, H., Gundestrup, N. and **Boggild, C.E.** 2002: Glacier specific ablation rate derived by remote sensing measurements. *Geophysical Research Letters* 16, 10.1029/2002GLO15307.

Reinwarth, O. and **Escher-Vetter, H.** 1999: Mass balance of Vernagtferner, Austria, from 1964/65 to 1996/97: results for three sections and the entire glacier. *Geografiska Annaler* 81A, 743–51.

Röthlisberger, H. and **Lang, H.** 1987: Glacial hydrology. In Gurnell, A.M. and Clark, M.J., editors, *Glacio-fluvial sediment transfer. An Alpine perspective,* New York: Wiley, 207–84.

Sauberer, F. 1955: Zur Abschätzung der Globalstrahlung in verschiedenen Höhenstufen. *Wetter und Leben* 7, 22–29.

Sauberer, F. and **Dirmhirn, I.** 1952: Der Strahlungshaushalt horizontaler Gletscherflächen auf dem Hohen Sonnblick. *Geografiska Annaler* 34, 261–90.

Schreider, T. and **Jansson, P.** 2004: Internal accumulation in firn and its significance for the mass balance of Storglaciären, Sweden. *Journal of Glaciology* 50, 25–34.

Schreider, S.Y., Whetton, P.H., Jakeman, A.J. and **Pittock, A.B.** 1997: Runoff modelling for snow-affected catchments in the Australian alpine region, eastern Victoria. *Journal of Hydrology* 200, 1–23.

Seidel, K. and **Martinec, J.** 1993: Operational snow cover mapping by satellites and real time runoff forecasts. In Young, G.J., editor, *Snow and glacier hydrology,* Proceedings of the Kathmandu Symposium 1992, Wallingford: IAHS Publication 218, 123-32.

Singh, P. and **Kumar, N.** 1996: Determination of snowmelt factor in the Himalayan region. *Hydrological Sciences Journal* 41, 301–10.

Smeets, P., Duynkerke, P.G. and **Vugts, H.F.** 1998: Turbulence characteristics of the stable boundary layer over a mid-latitude glacier. Part i: a combination of katabatic and large-scale forcing. *Boundary-Layer Meteorology* 87, 117–45.

Streten, N.A. and **Wendler, G.** 1968: The midsummer heat balance of an Alaskan maritime glacier. *Journal of Glaciology* 7, 431–40.

Sverdrup, H.U. 1935: Scientific results of the Norwegian-Swedish Spitzbergen Expedition in 1934. Part IV. The ablation on Isachsen's plateau and on the Fourteenth of July Glacier in relation to radiation and meteorological conditions. *Geografiska Annaler* 17, 145–66.

— 1936: The eddy conductivity of the air over a smooth snow field. *Geofysiske Publikasjoner* 11, 5–69.

Tangborn, W.V. 1984: Prediction of glacier derived runoff for hydro-electric development. *Geografiska Annaler* 66A, 257–65.

Trabant, D.C. and **Mayo, L.R.** 1985: Estimation and effects of internal accumulation on five different glaciers in Alaska. *Annals of Glaciology* 6, 113–17.

Ujihashi, Y., Takase, N., Ishida, H. and **Hibobe, E.** 1994: Distributed snow cover model for a mountainous basin. In Jones, H.G., Davies, T.D., Ohmura, A. and Morris, E.M., editors, *Snow and ice covers: interactions with the atmosphere and ecosystems,* Proceedings of the Yokohama Symposium 1993, Wallingford: IAHS Publication 223, 153–62.

van de Wal, R.S.W. and **Russell, A.J.** 1994: A comparison of energy balance calculations, measured ablation and meltwater runoff near Søndre Strømfjord, West Greenland. *Global Planetary Change* 9, 29–38.

van de Wal, R.S.W., Oerlemanns, J. and **Hage, J.C.** 1992: A study of ablation variations on the tongue of Hintereisferner, Austrian Alps. *Journal of Glaciology* 38, 319–24.

van den Broeke, M. 1996: Characteristics of the lower ablation zone of the west Greenland ice sheet for energy-balance modelling. *Annals of Glaciology* 23, 160–66.

— 1997: Structure and diurnal variation of the atmospheric boundary layer over a mid-latitude glacier in summer. *Boundary-Layer Meteorology* 83, 183–205.

van der Avoird, E. and **Duynkerke, P.G.** 1999: Turbulence in a katabatic flow. Does it resemble turbulence in stable boundary layers over flat surfaces. *Boundary-Layer Meteorology* 92, 39–66.

Varley, M.J. and **Beven, K.J.** 1996: Modelling solar radiation in steeply sloping terrain. *Journal of Climatology* 16, 93–104.

Wagner, H.P. 1980a: Strahlungshaushaltsuntersuchungen an einem Ostalpengletscher während der Hauptablationsperiode Teil I: Kurzwellige Strahlungsbilanz. *Archiv für Meteorologie, Geophysik und Bioklimatologie* B(27), 297–324.

— 1980b: Strahlungshaushaltsuntersuchungen an einem Ostalpengletscher während der Hauptablationsperiode Teil II: Langwellige Strahlung und Strahlungsbilanz. *Archiv für Meteorologie, Geophysik und Bioklimatologie* B(28), 41–62.

Wagnon, P., Ribstein, P., Francou, B. and **Pouyaud, B.** 1999: Annual cycle of the energy balance of Zongo Glacier, Cordillera Real, Bolivia. *Journal of Geophysical Research* 104, 3907–23.

Walcher, J. 1773: Nachrichten von den Eisbergen in Tyrol. Wien, 99 pp.

Wallén, C.C. 1949: The shrinkage of the Kårsa Glacier and its probable meteorological causes. *Geografiska Annaler* 1-2, 275–91.

Warren, S.G. 1982: Optical properties of snow. *Reviews of Geophysics and Space Physics* 20, 67–89.

Warren, S.G. and **Wiscombe, W.J.** 1980: A model for the spectral albedo of snow. II. Snow containing atmospheric aerosols. *Journal of Atmoheric Science* 37, 2734–45.

Webb, E.K. 1970: Profile relationships: the log-linear range, and extension to strong stability. *Quartely Journal of the Royal Meteorological Society* 96, 67–90.

Wendler, G. 1975: A note on the advection of warm air towards a glacier. A contribution to the International Hydrological Decade. *Zeitschrift für Gletscherkunde und Glazialgeologie* 10, 199–205.

Wesley, M.L. and **Lipschutz, R.C.** 1976: A method for estimation hourly averages of diffuse and direct solar radiation under a layer of scattered clouds. *Solar Energy* 18, 467–73.

Willis, I.C., Arnold, N.S. and **Brock, B.W.** 2002: Effect of snowpack removal on energy balance, melt and runoff in a small supraglacial catchment. *Hydrological Processes* 16, 2721–49.

Willis, I.C., Sharp, M.J. and **Richards, K.S.** 1993: Studies of the water balance of Midtdalsbreen, Hardangerjökulen, Norway. I. The calculation of surface water inputs from basic meteorological data. *Zeitschrift für Gletscherkunde und Glazialgeologie* 27/28, 97–115.

Winther, J., Elvehoy, H., Bøggild, C., Sand, K. and **Liston, G.** 1996: Melting, runoff and the formation of frozen lakes in a mixed snow and blue-ice field in Dronning Maud Land, Antarctica. *Journal of Glaciology* 42, 271–78.

World Meterology Organization (WMO) 1986: Intercomparison of models for snowmelt runoff. *Operational Hydrology Report* 23 (WMO no. 646).

Zuo, Z. and **Oerlemans, J.** 1996: Modelling albedo and specific balance of the Greenland ice sheet: calculations for the Søndre Strømfjord transect. *Journal of Glaciology* 42, 305–33.